

第八届手征有效场论研讨会，2023年10月28-30日



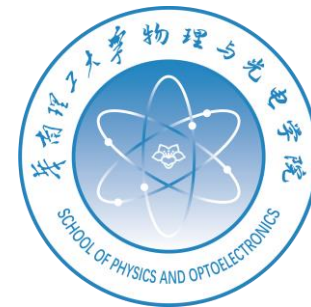
中高能重离子碰撞中核结团和超核结团产生

冯兆庆

华南理工大学物理与光电学院

*Email: fengzhq@scut.edu.cn





报告内容

- 中高能重离子碰撞中核结团和超核结团产生
- LQMD输运模型
- 原子核碎裂反应和超核形成
- 总结与展望

一、中高能重离子碰撞中核结团和超核结团产生



1. 中能重离子碰撞(30A MeV–5A GeV)核结团和超核结团实验进展

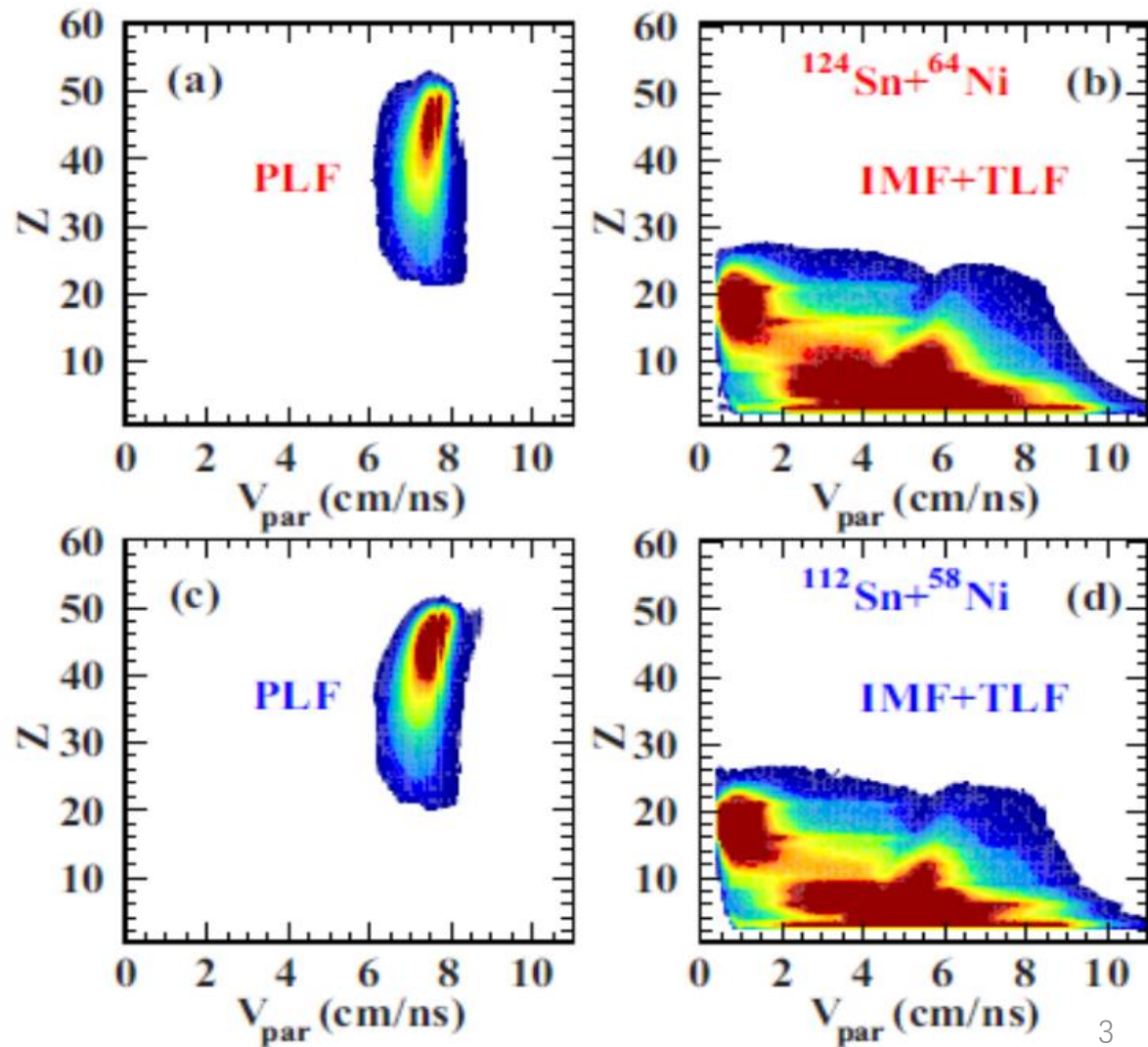
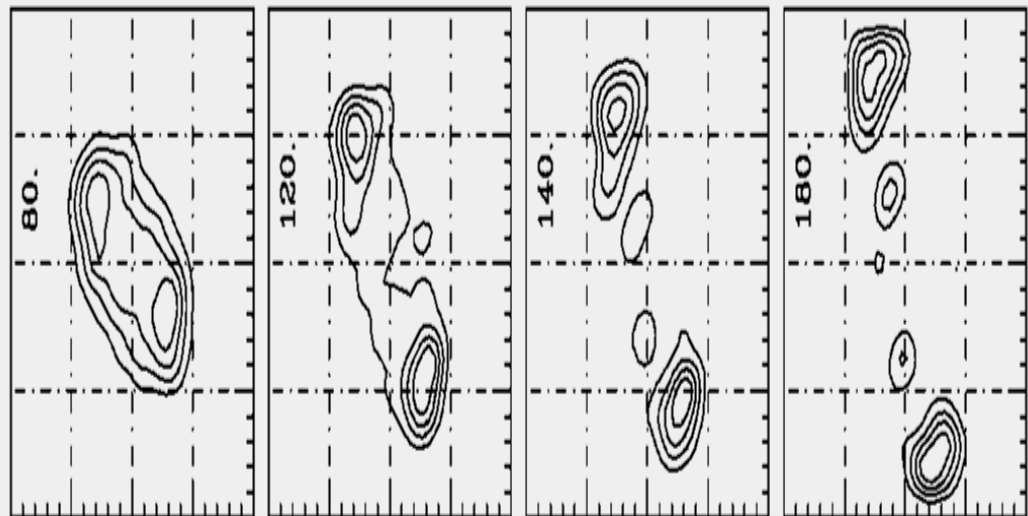
P. Russotto *et al.*, PRC 91, 014610 (2015)

Experiments:

INDRA (GANIL), CHIMERA (LNS), NSCL (MSU)

SSC and CSR(HIRFL), FOPI and HADES (GSI) ...

密度演化等高图



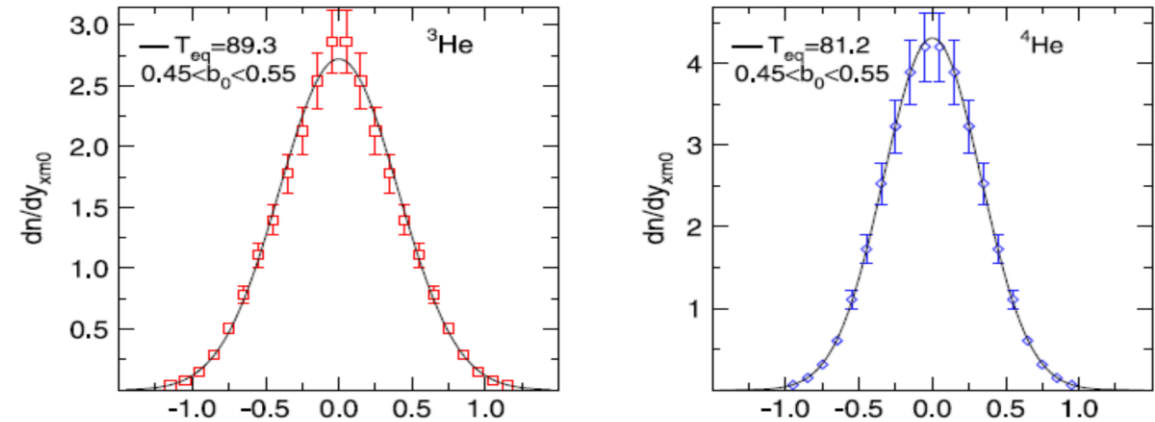
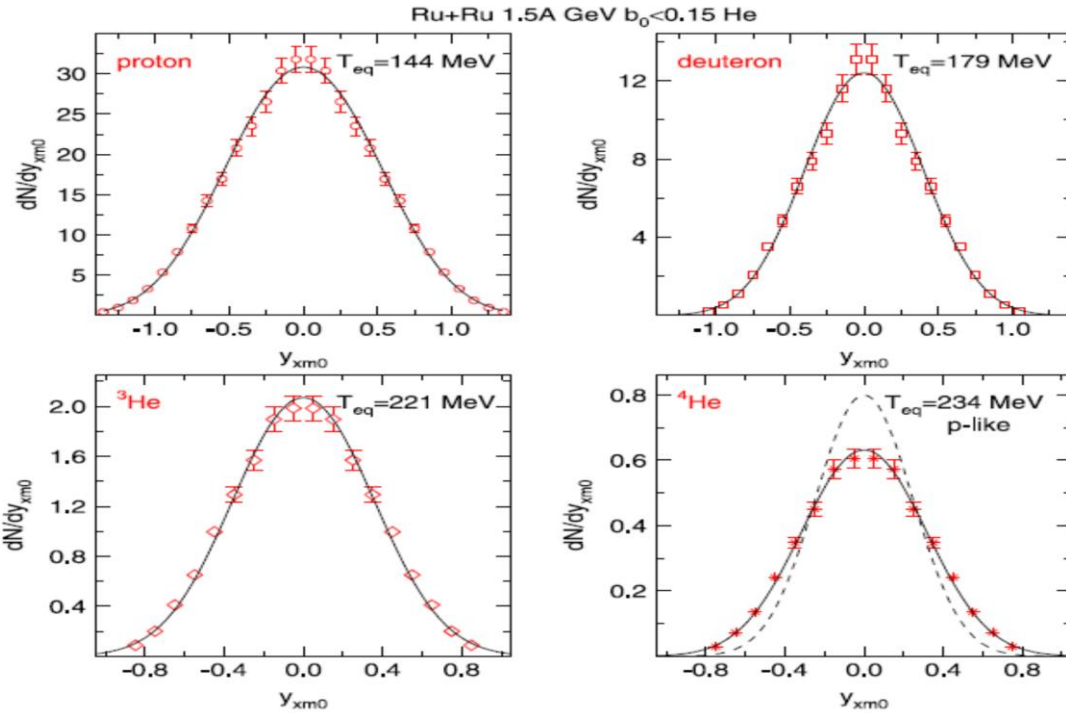
Cluster production measurement at FOPI



Systematics of central heavy ion collisions in the 1 A GeV regime

FOPI Collaboration

Au+Au 0.4A GeV

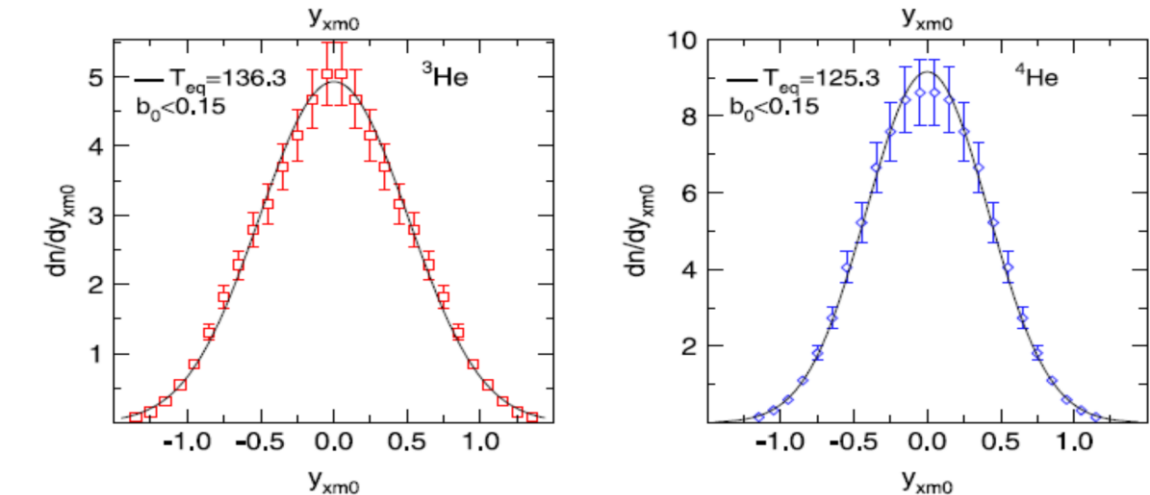


Multiplicities and charge balance for Au + Au at $E/A = 0.15$ GeV and $b_0 < 0.15$.

Z = 1	59.9 ± 3.0	p	24.1 ± 1.2	Z = 2	25.0 ± 1.8	${}^3\text{He}$	8.4 ± 0.9
		d	20.4 ± 1.4			${}^4\text{He}$	16.6 ± 1.7
		t	15.1 ± 1.5				
		Li	5.0 ± 0.5	Be	1.69 ± 0.17		
		B	1.44 ± 0.15	C	0.90 ± 0.09		
		N	0.50 ± 0.05	O	0.26 ± 0.03		

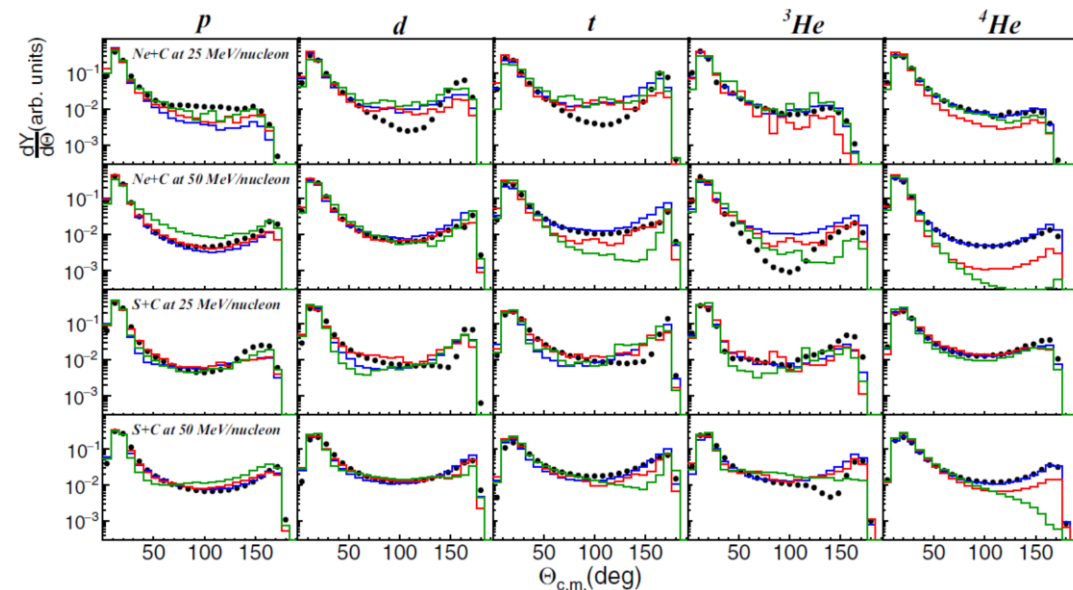
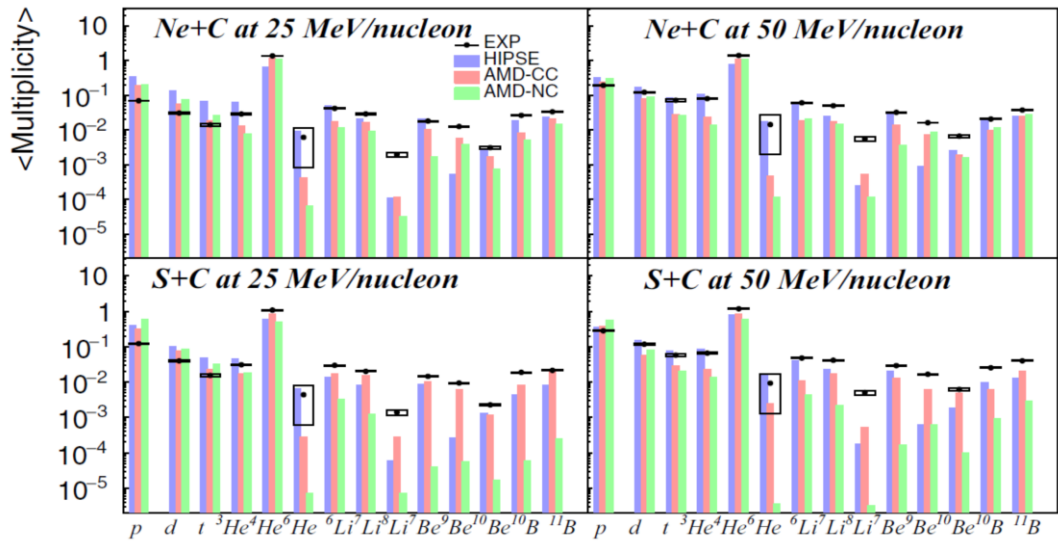
Multiplicities and charge balance for Ni + Ni at $E/A = 0.25$ GeV and $b_0 < 0.15$.

Z = 1	34.9 ± 1.8	p	19.2 ± 1.0	Z = 2	9.0 ± 0.7	${}^3\text{He}$	3.24 ± 0.33
		d	10.5 ± 0.8			${}^4\text{He}$	5.79 ± 0.58
		t	5.1 ± 0.5				
		Li	0.91 ± 0.09	Be	0.26 ± 0.03		
		B	0.10 ± 0.01				



Cluster production measurement

at FOPI INDRA-FAZIA

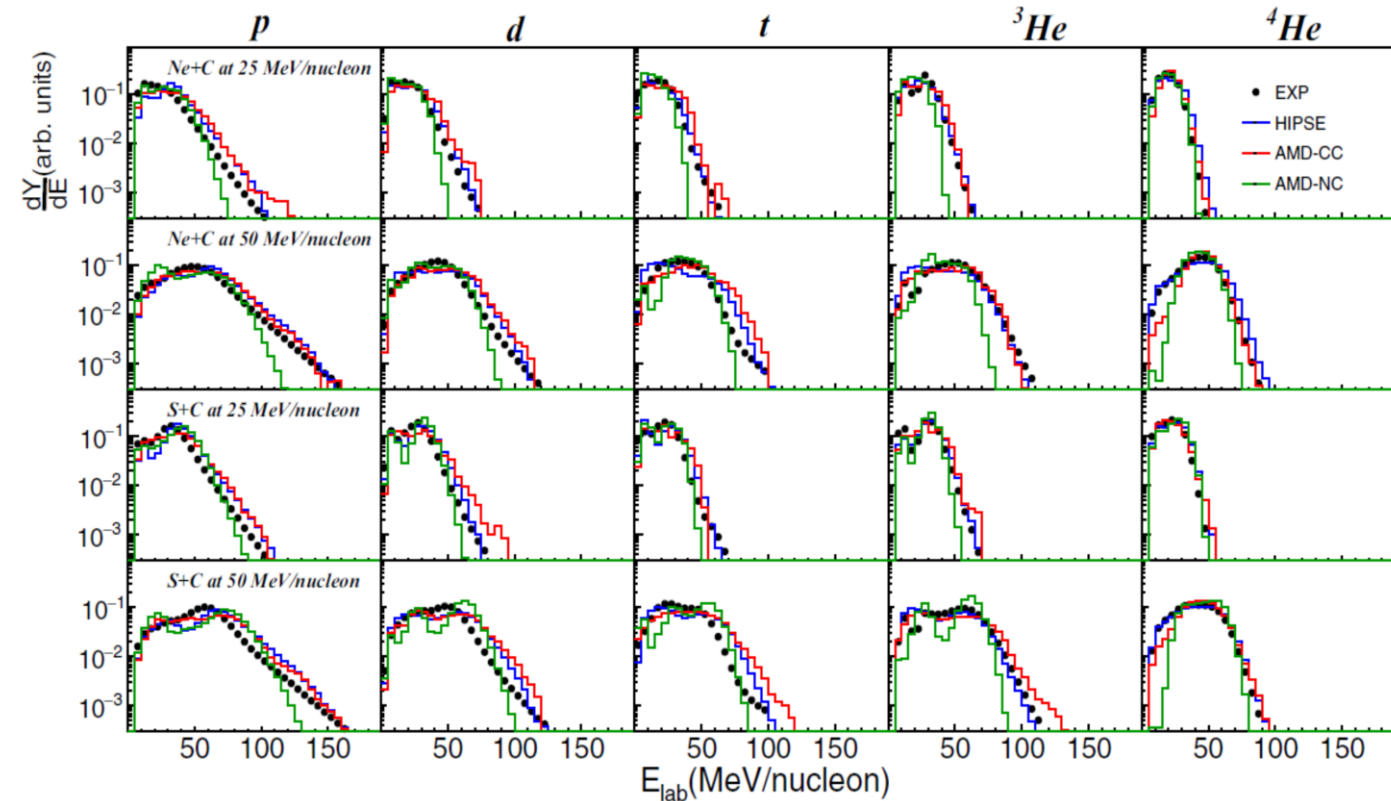


Featured in Physics

Examination of cluster production in excited light systems at Fermi energies from new experimental data and comparison with transport model calculations

C. Frosin^{1,2,*}, S. Piantelli,² G. Casini,² A. Ono,³ A. Camaiani,⁴ L. Baldesi,² S. Barlini,^{1,2} B. Borderie,⁵ R. Bougault,⁶ C. Ciampi,^{1,2} M. Cicerchia,⁷ A. Chbihi,⁸ D. Dell'Aquila,^{9,10} J. A. Dueñas,¹¹ D. Fabris,¹² Q. Fable,¹³ J. D. Frankland,⁸ T. Génard,⁸ F. Gramegna,⁷ D. Gruyer,⁶ M. Henri,⁸ B. Hong,^{14,15} M. J. Kweon,¹⁶ S. Kim,¹⁷ A. Kordyasz,¹⁸ T. Kozik,¹⁹ I. Lombardo,^{20,21} O. Lopez,⁶ T. Marchi,⁷ K. Mazurek,²² S. H. Nam,^{14,15} J. Lemarié,⁸ N. LeNeindre,⁶ P. Ottanelli,² M. Parlog,^{6,23} J. Park,^{14,15} G. Pasquali,^{1,2} G. Poggi,^{1,2} A. Rebillard-Soulié,⁶ B. H. Sun,²⁴ A. A. Stefanini,^{1,2} S. Terashima,²⁴ S. Upadhyaya,¹⁹ S. Valdré,² G. Verde,^{20,13} E. Vient,⁶ and M. Vigilante^{25,26}

(INDRA-FAZIA Collaboration)

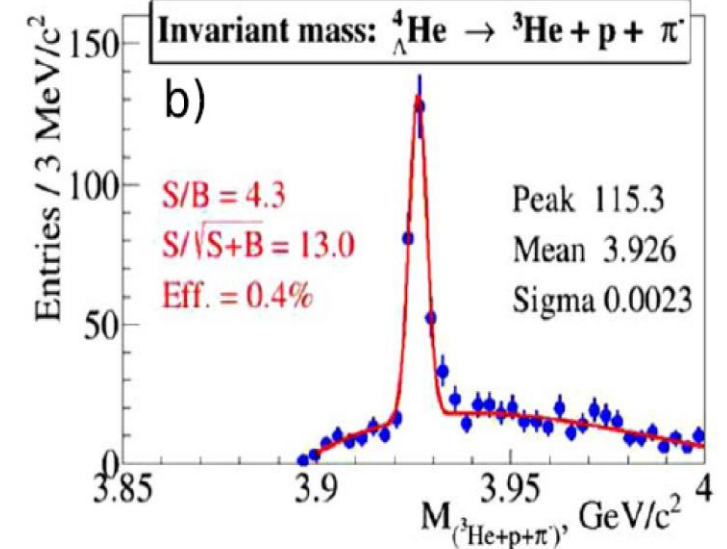
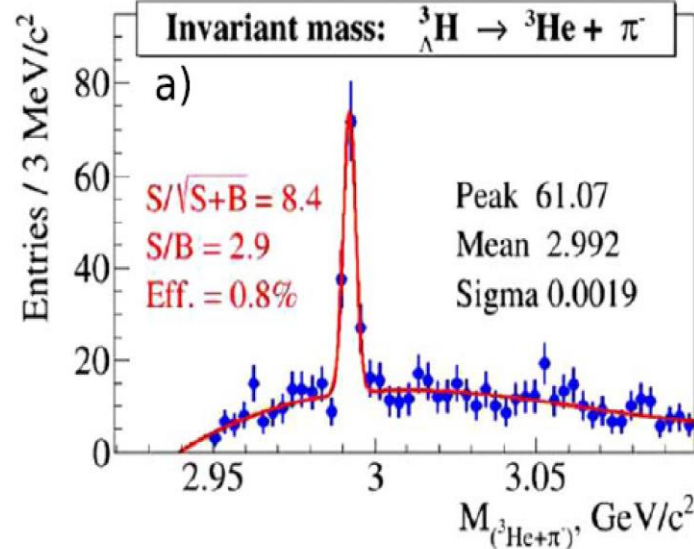
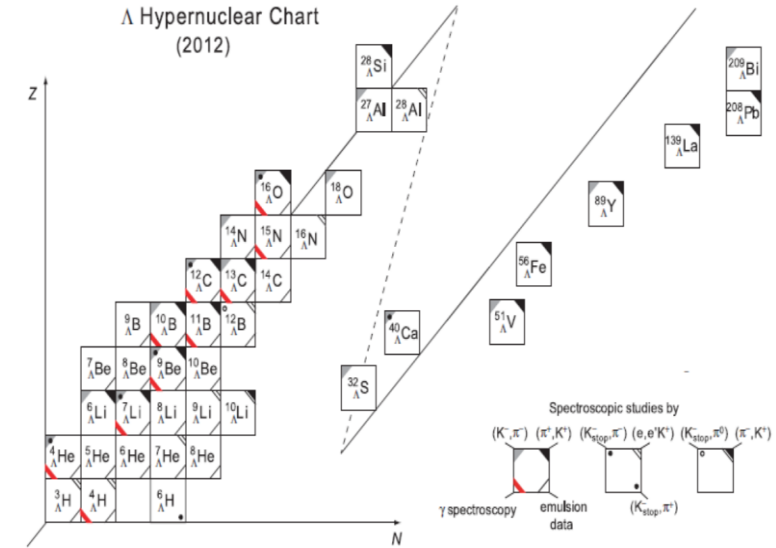
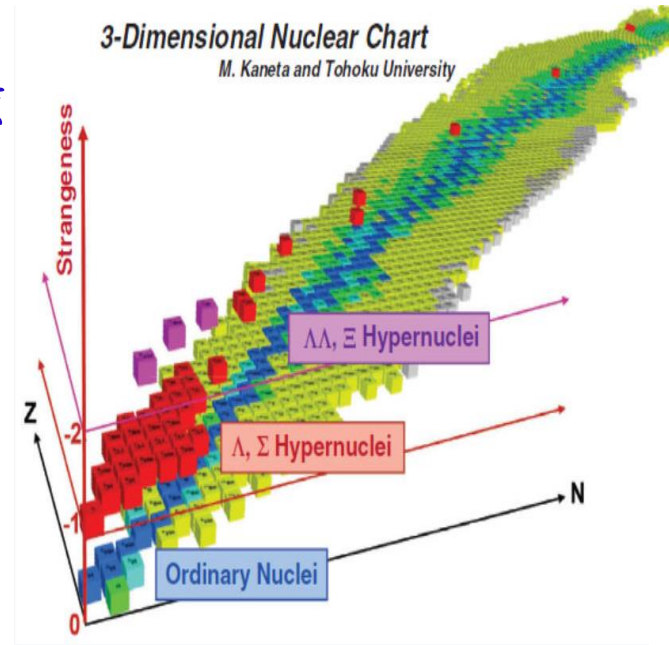
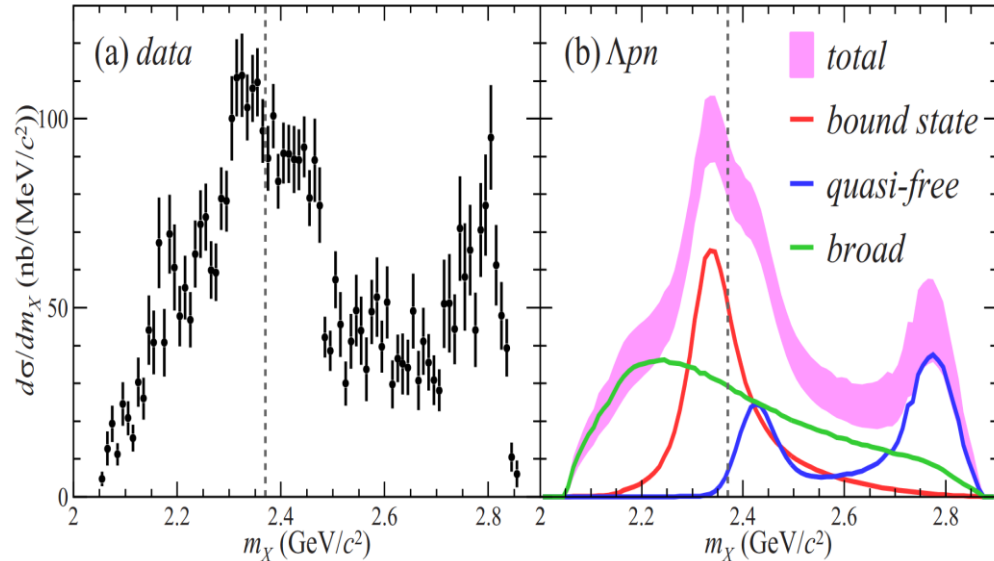


重离子碰撞产生超核

1. 极端丰中子或丰质子超核产生和谱学性质
2. 奇特超核产生 ($S=-2$) $\Lambda\Lambda$ X和 Ξ X
3. 核物质中 Λ - Λ 和 Ξ -N相互作用

PHYSICAL REVIEW C **102**, 044002 (2020)

Observation of a $\bar{K}NN$ bound state in the ${}^3\text{He}(K^-, \Delta p)n$ reaction

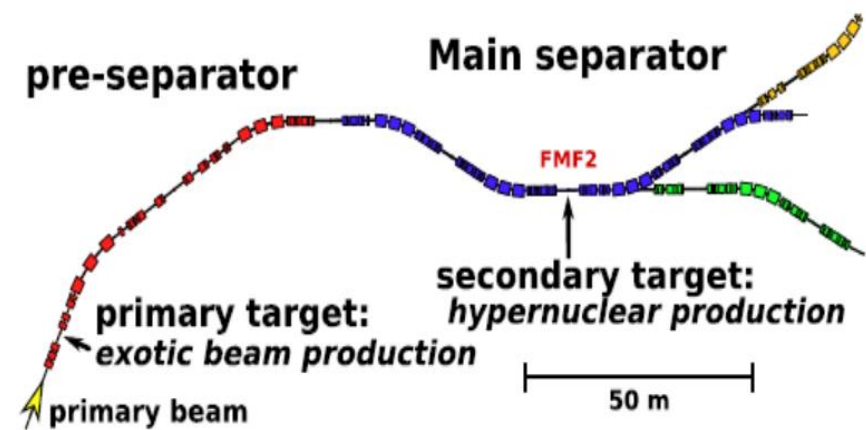


德国GSI产生丰质子/丰质子超核

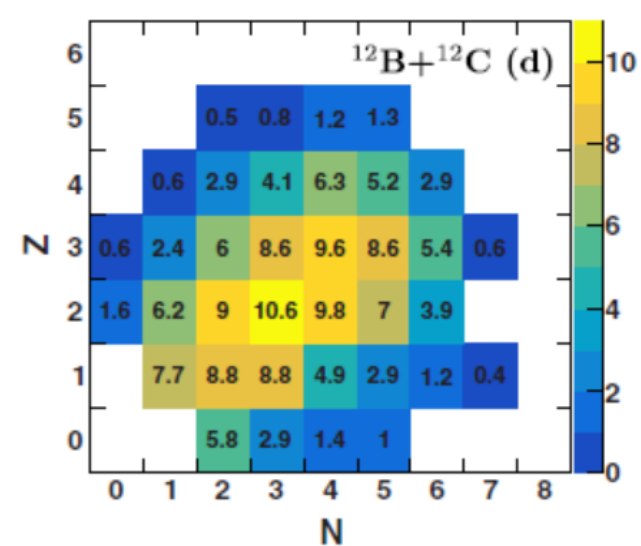
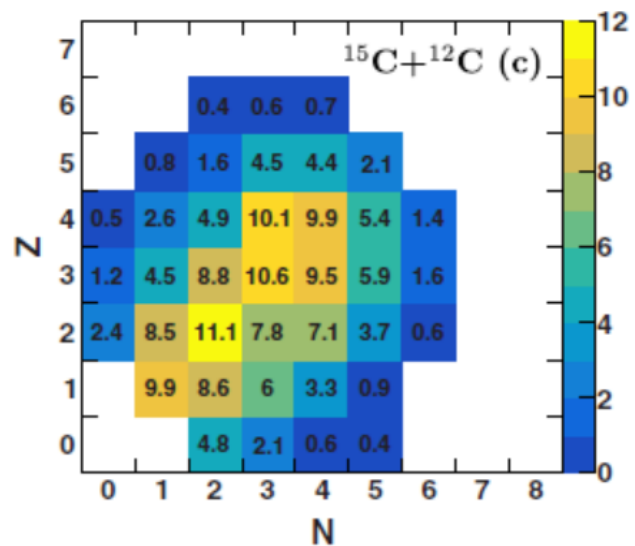
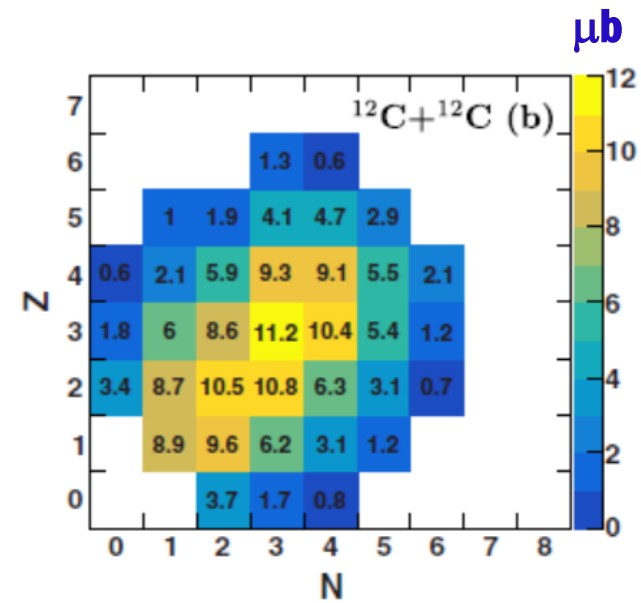
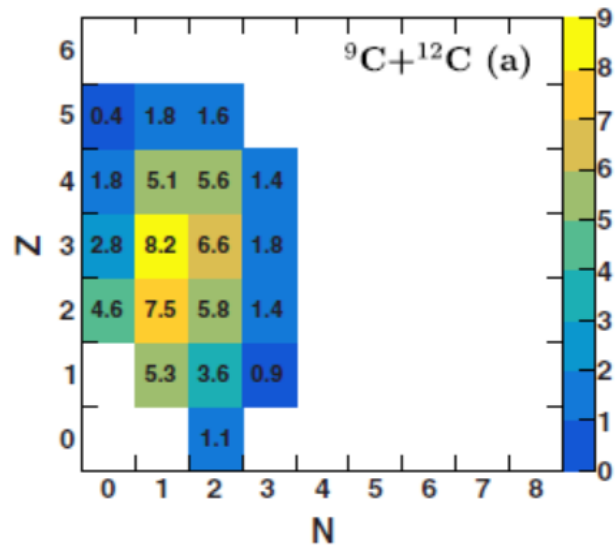
实验条件分析

C. Rappold, J. López-Fidalgo, PRC 94,

044616 (2016)

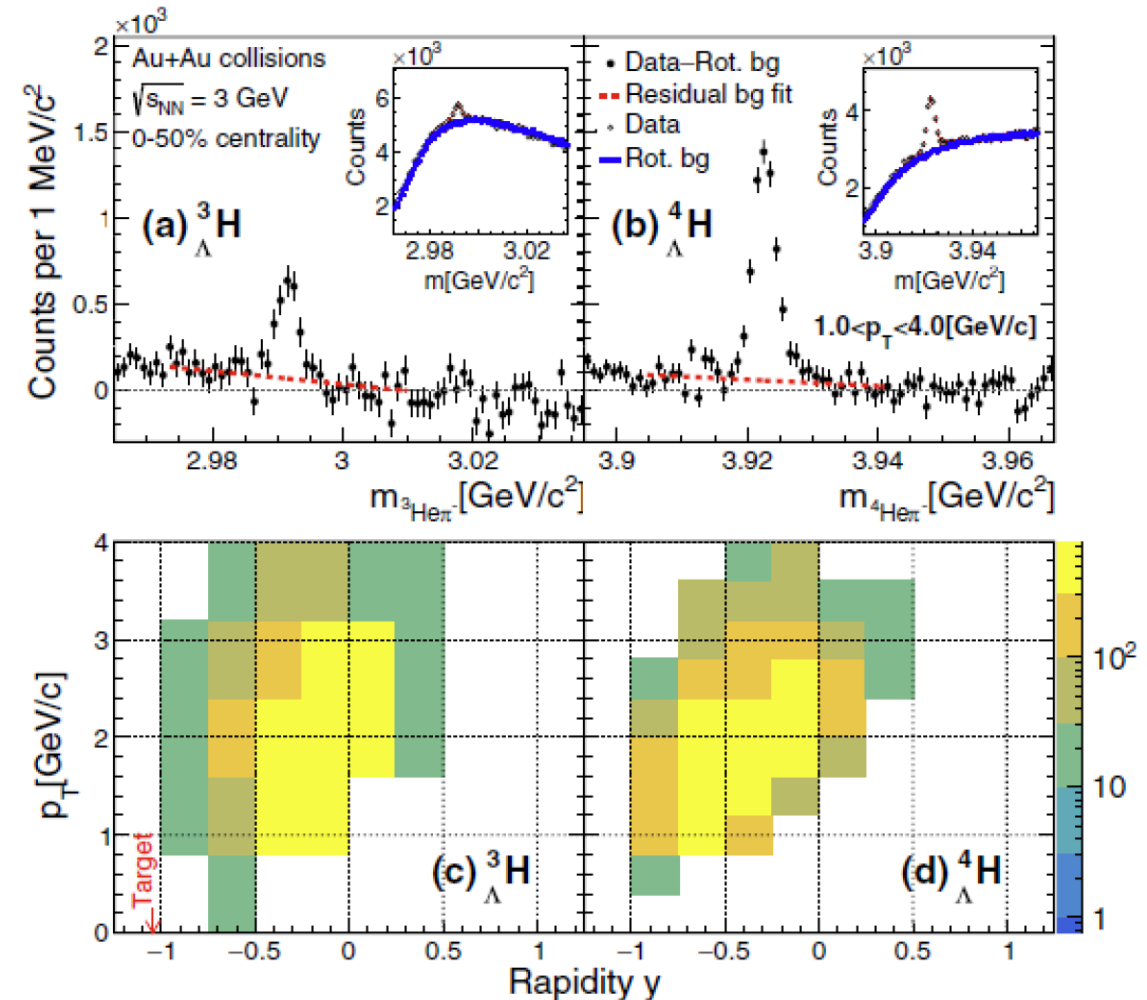
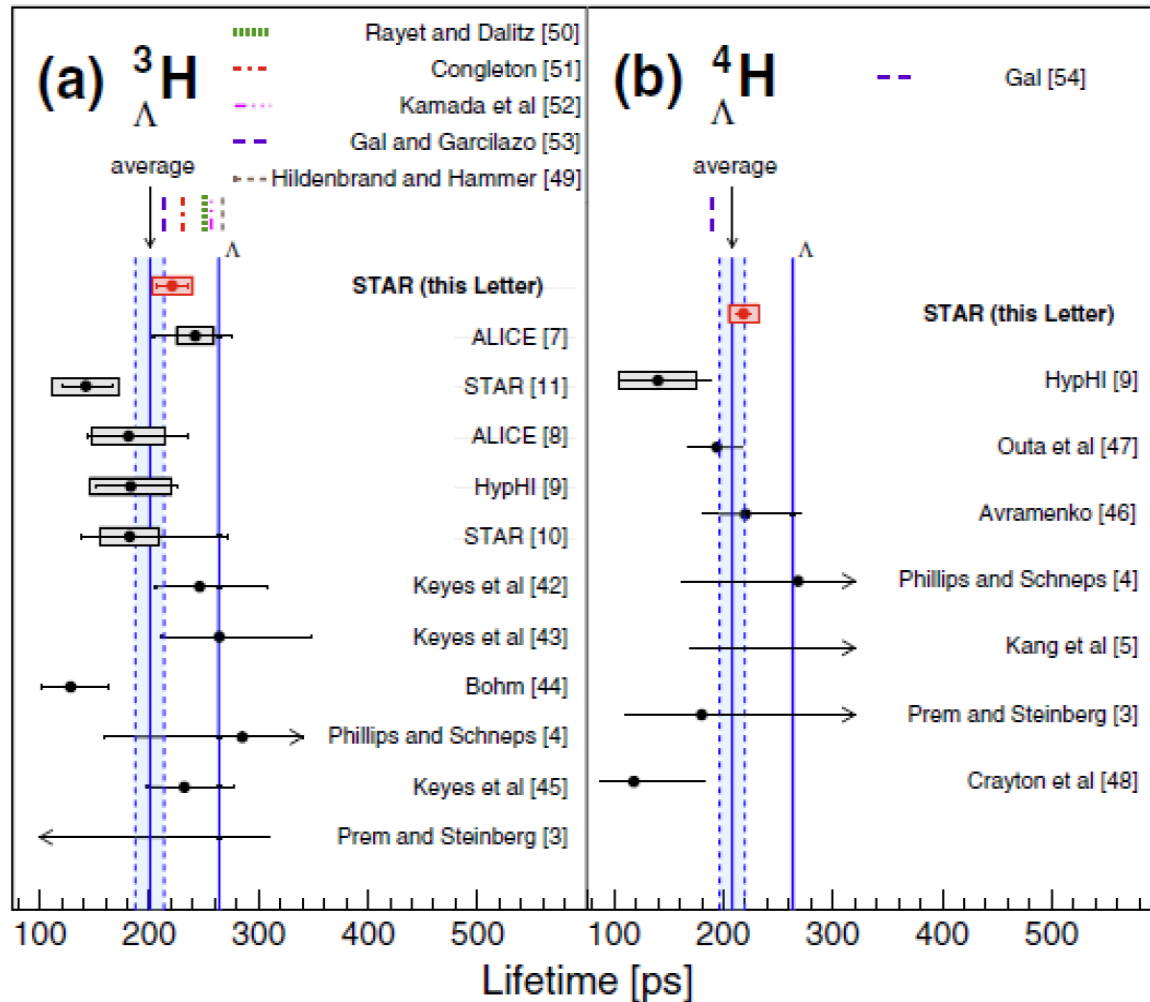


Λ -hypernuclei

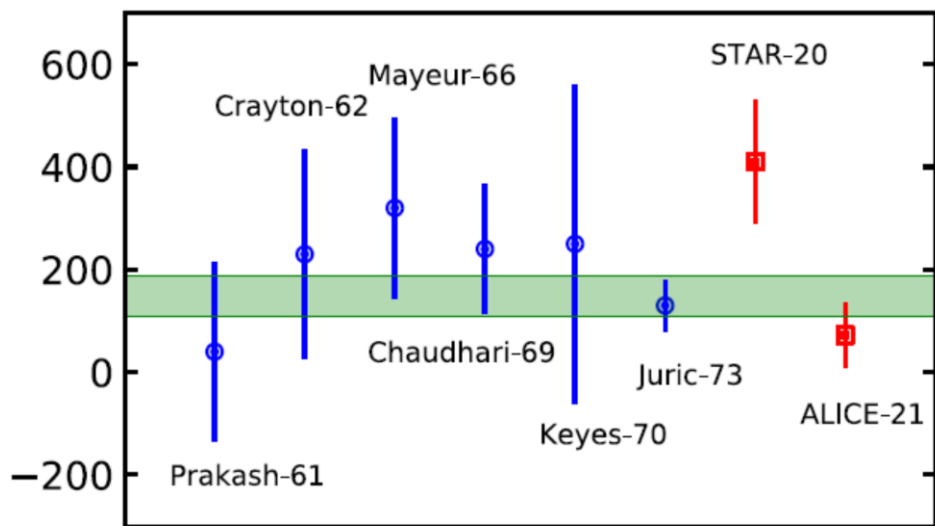


相对论重离子对撞机上超核寿命测量

Hypernuclide ${}^3_{\Lambda}\text{H}$ and ${}^4_{\Lambda}\text{H}$ measured by STAR Collaboration (Phys. Rev. Lett. 128, 202301 (2022))



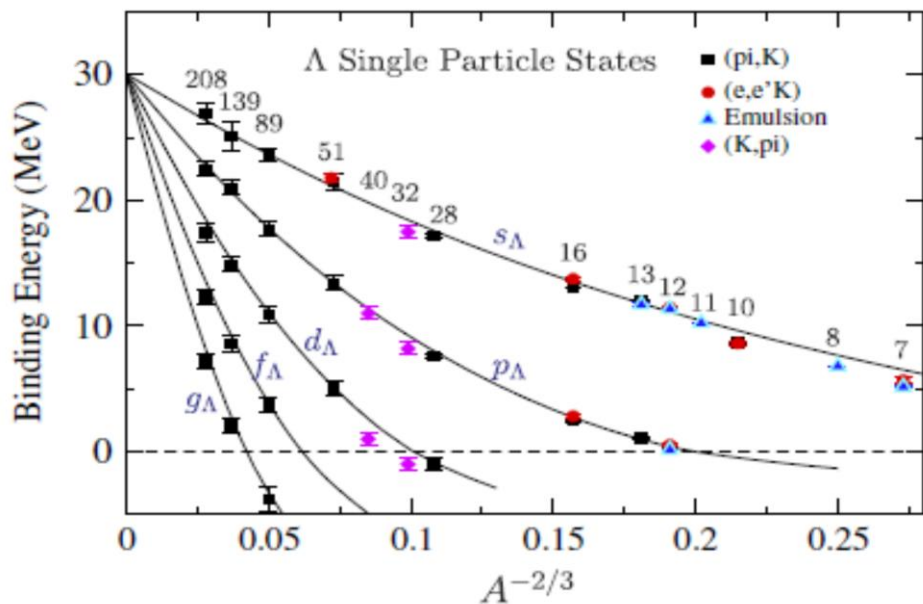
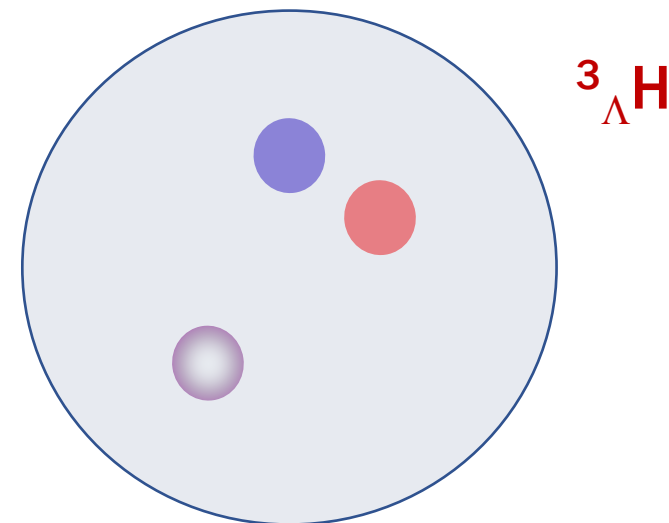
超氦核半径和结合能



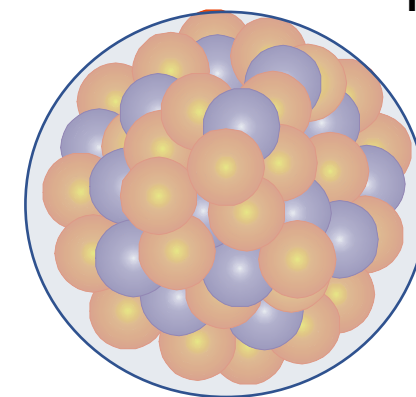
$$B_{\Lambda} = 72^{+63}_{-36} \text{ keV}$$

$$R \sim 10 \text{ fm}$$

$$B_{\Lambda} = 148 \pm 40 \text{ keV}$$



${}^{208}\text{Pb}$, $R \sim 7 \text{ fm}$



Millener, D. J., C. B. Dover, and A. Gal, 1988, Phys. Rev. C 38, 2700

中子星物质相结构

VOLUME 75, NUMBER 6

PHYSICAL REVIEW LETTERS

7 AUGUST 1995

Probing the Nuclear Liquid-Gas Phase Transition

J. Pochodzalla,¹ T. Möhlenkamp,² T. Rubehn,¹ A. Schüttauf,³ A. Wörner,¹ E. Zude,¹ M. Begemann-Blaich,¹ Th. Blaich,⁴ H. Emling,¹ A. Ferrero,^{5,*} C. Gross,¹ G. Immé,⁶ I. Iori,⁵ G. J. Kunde,^{1,†} W. D. Kunze,¹ V. Lindenstruth,^{1,4} U. Lynen,¹ A. Moroni,⁵ W. F. J. Müller,¹ B. Ocker,³ G. Raciti,⁶ H. Sann,¹ C. Schwarz,¹ W. Seidel,² V. Serfling,³ J. Stroth,¹ W. Trautmann,¹ A. Trzcinski,⁷ A. Tucholski,⁷ G. Verde,⁵ and B. Zwieglinski⁷

PHYSICAL REVIEW C **102**, 045801 (2020)

Editors' Suggestion Featured in Physics

Fast neutrino cooling of nuclear pasta in neutron stars: Molecular dynamics simulations

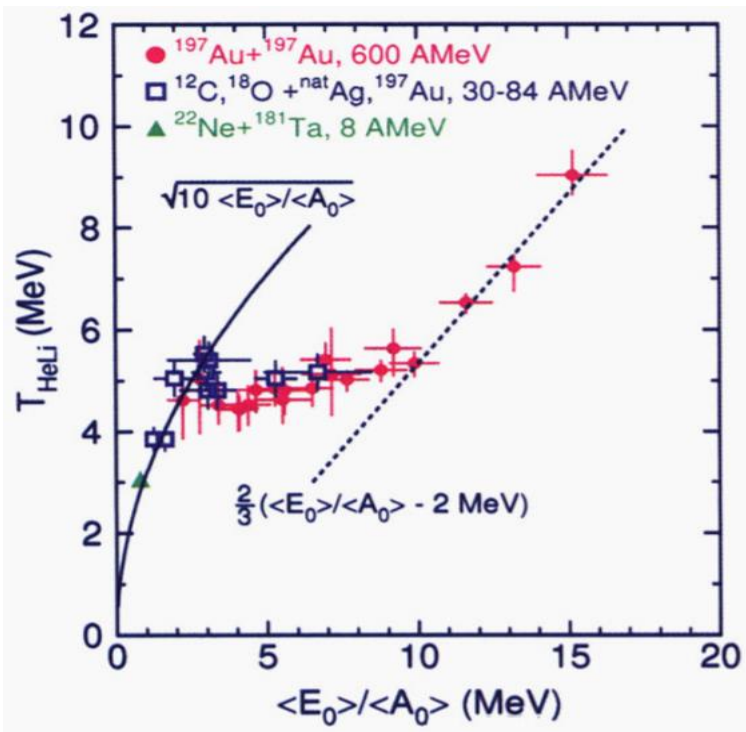
Zidu Lin¹, Matthew E. Caplan,² Charles J. Horowitz,³ and Cecilia Lunardini¹

¹Department of Physics, Arizona State University, 450 East Tyler Mall, Tempe, Arizona 85287-1504, USA

²Department of Physics, Illinois State University, Normal, Illinois 61790, USA

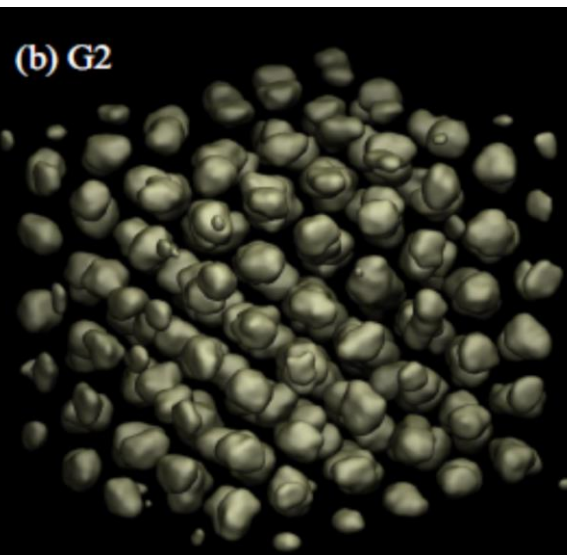
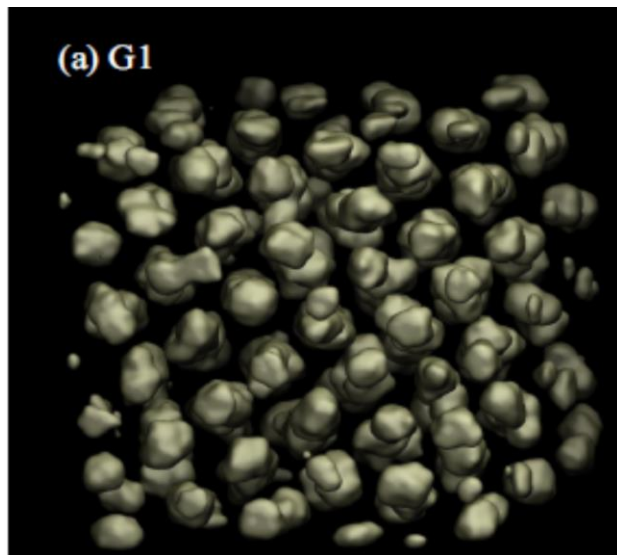
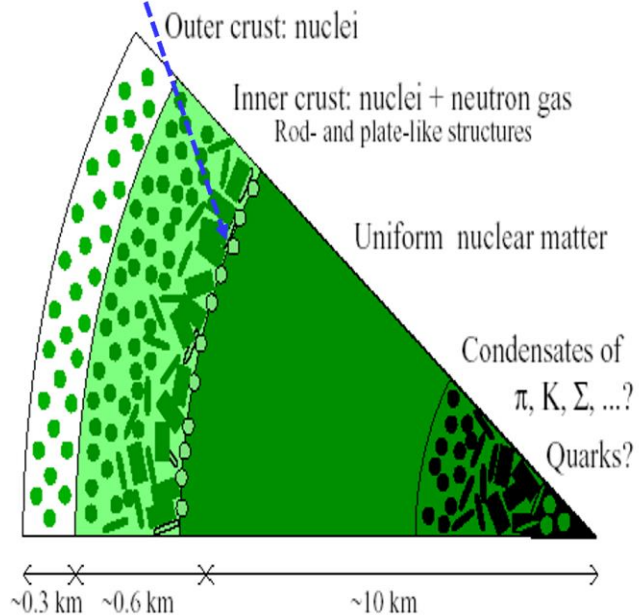
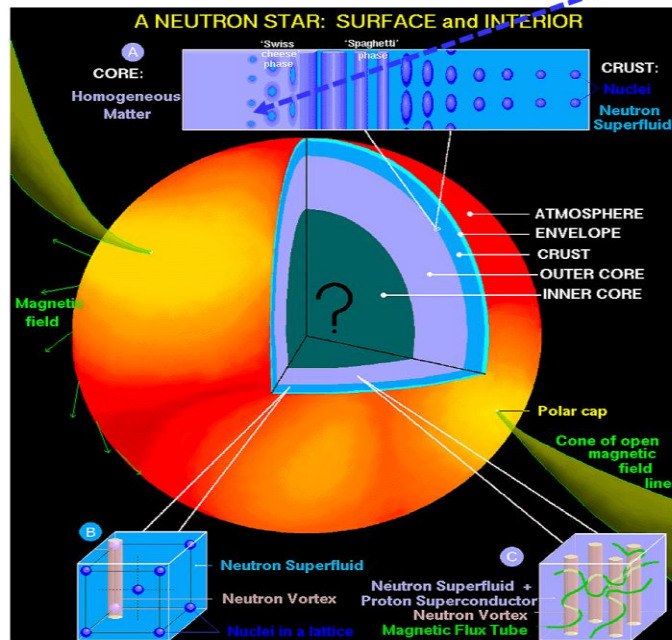
³Center for the Exploration of Energy and Matter and Department of Physics, Indiana University, Bloomington, Indiana 47405, USA

(Received 18 June 2020; accepted 17 August 2020; published 6 October 2020)



J. M. Lattimer and M. Prakash, Science 304, 536 (2004)

芯-内壳的转换密度

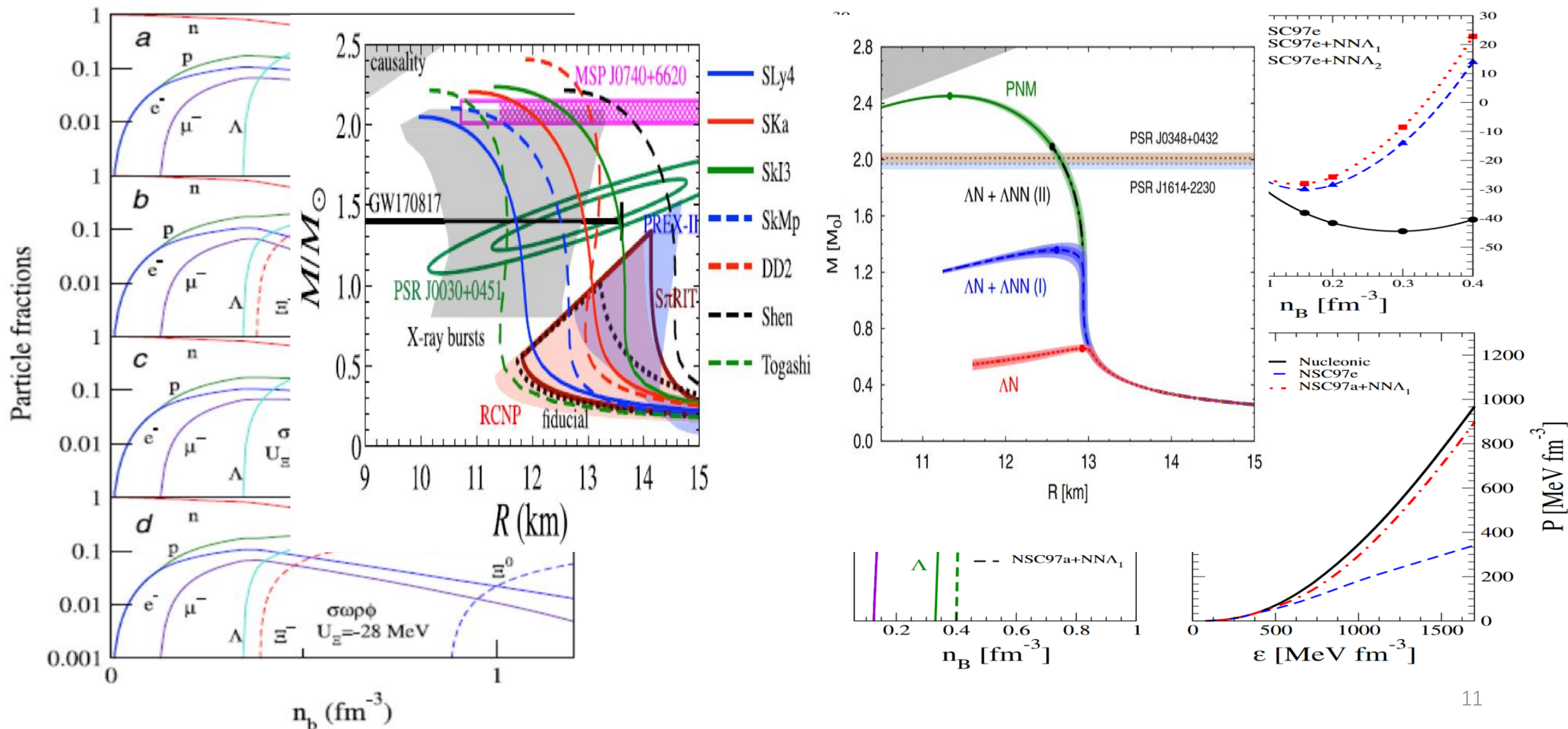


中子星物质中的超子成分

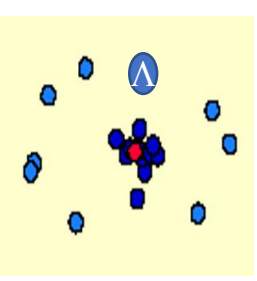
S. Weissenborn, D. Chatterjee, J. Schaffner-Bielich, Nucl. Phys. A 881, 62 (2012)

W. Z. Jiang, R. Y. Yang, and D. R. Zhang, Phys. Rev. C 87, 064314 (2013)

Diego Lonardonì, Alessandro Lovato, Stefano Gandolfi, and Francesco Pederiva, Phys. Rev. Lett. 114, 092301 (2015)



2. 核结团和超核碎片构造和动力学

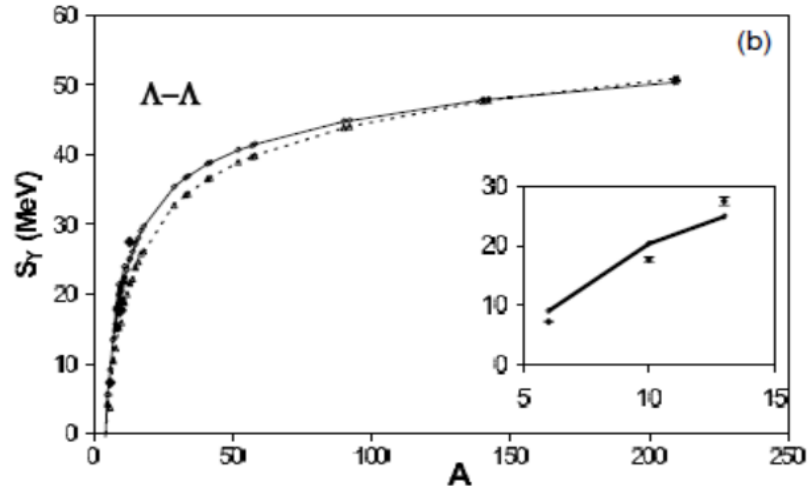
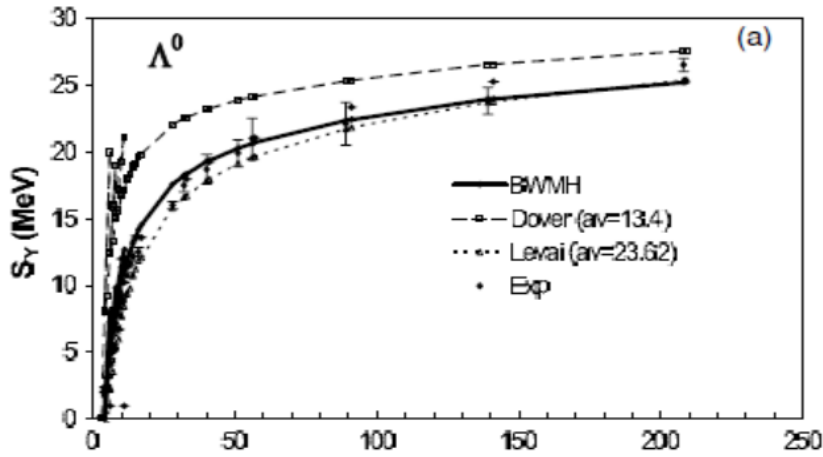


1) Classical coalescence approach in phase space for nuclides of $Z > 2$ combined with the GEMINI decay code (minimum spanning tree (MST) procedure)

$$|r_i - r_j| \leq 3 \text{ fm}, |r_i - r_Y| \leq 4.5 \text{ fm}, |p_i - p_j| \leq 0.3 \text{ GeV}/c$$

C. Samanta et al, J. Phys. G: Nucl. Part. Phys. 32 (2006) 363

Binding energy: $E_B(Z_i, N_i) = \sum_j \sqrt{p_j^2 + m_j^2} - m_j$



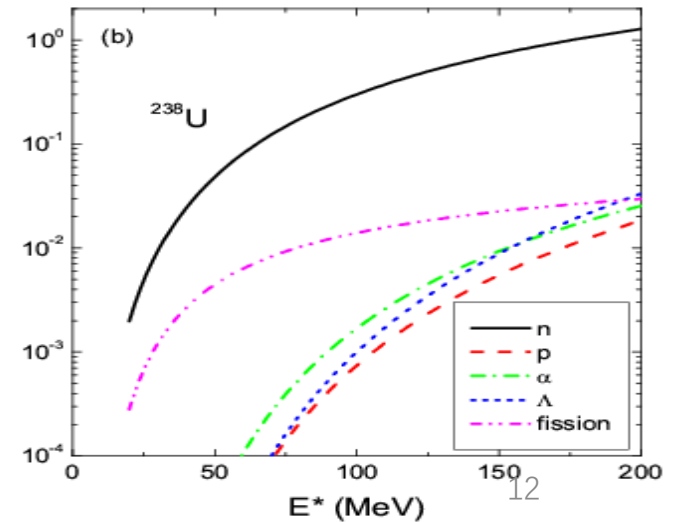
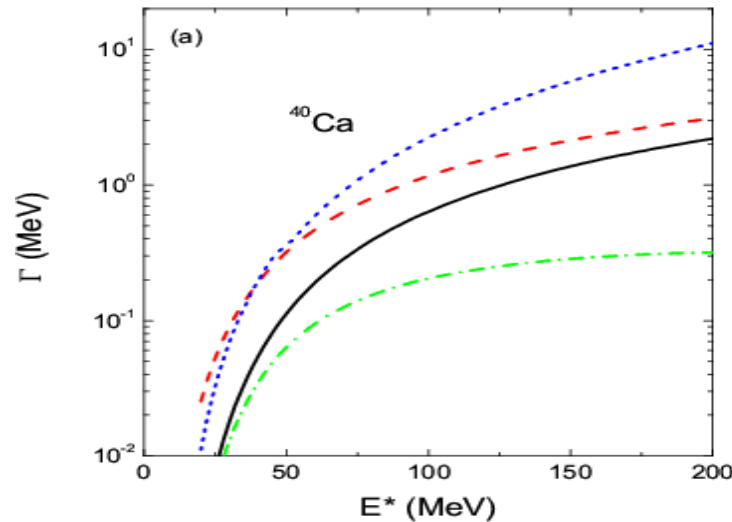
Excitation energy $E^*(Z_\nu, N_\nu, nY)$

$$= E_B(Z_\nu, N_\nu, nY) - E_{LD}(Z_\nu, N_\nu, nY)$$

The decay of excited hypernucleus is described by the GEMINI code!

$$+ \frac{1}{2} \sum_{j,k,k \neq j} \int f_j(\mathbf{r}, \mathbf{p}, t) f_k(\mathbf{r}', \mathbf{p}', t) \times v(\mathbf{r}, \mathbf{r}', \mathbf{p}, \mathbf{p}') d\mathbf{r} d\mathbf{r}' d\mathbf{p} d\mathbf{p}'$$

$$+ \frac{1}{6} \sum_{j,k,l} \sum_{k \neq j, k \neq l, j \neq l} \int f_j(\mathbf{r}, \mathbf{p}, t) f_k(\mathbf{r}', \mathbf{p}', t) \times f_l(\mathbf{r}'', \mathbf{p}'', t) v(\mathbf{r}, \mathbf{r}', \mathbf{r}'', \mathbf{p}, \mathbf{p}', \mathbf{p}'') \times d\mathbf{r} d\mathbf{r}' d\mathbf{r}'' d\mathbf{p} d\mathbf{p}' d\mathbf{p}''$$

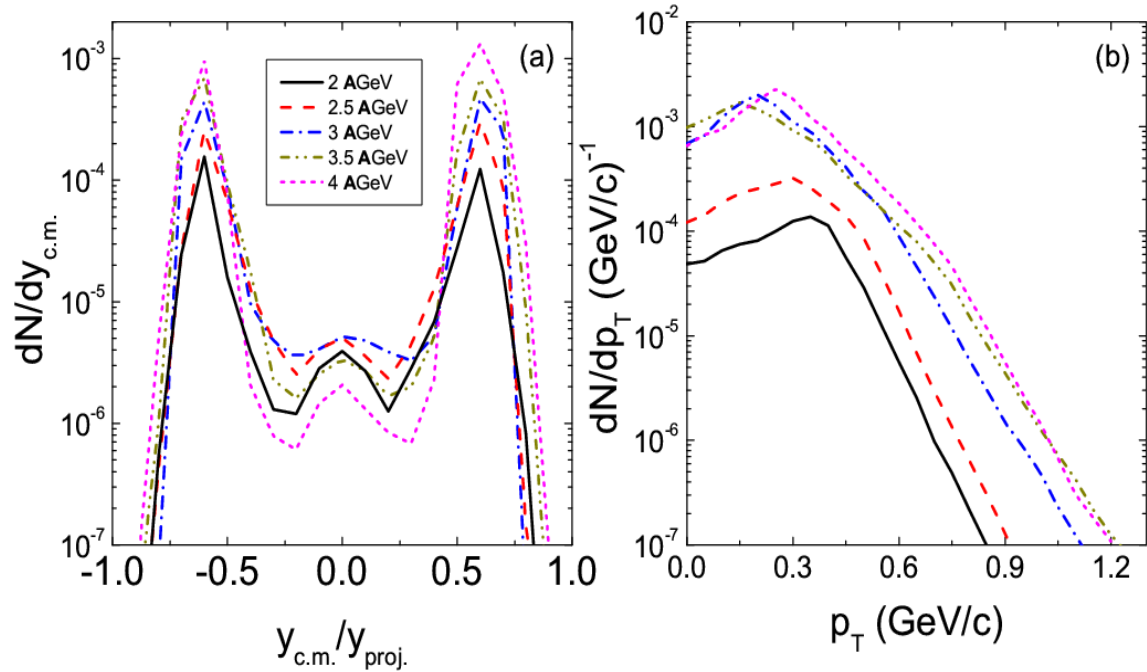


2) Wigner density approach for $Z \leq 2$

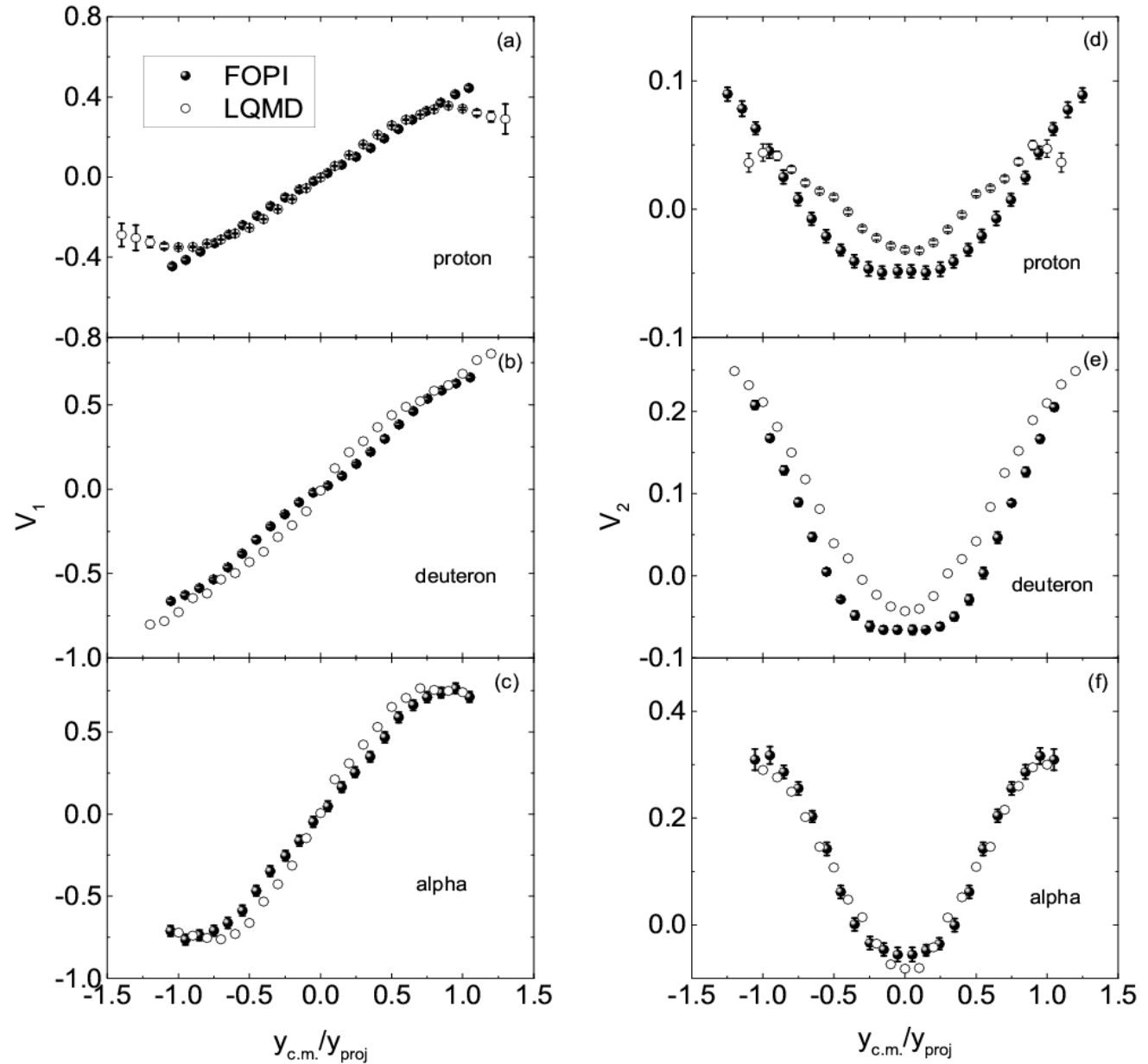
R. Mattiello et al., Phys. Rev. C 55, 1443 (1997)

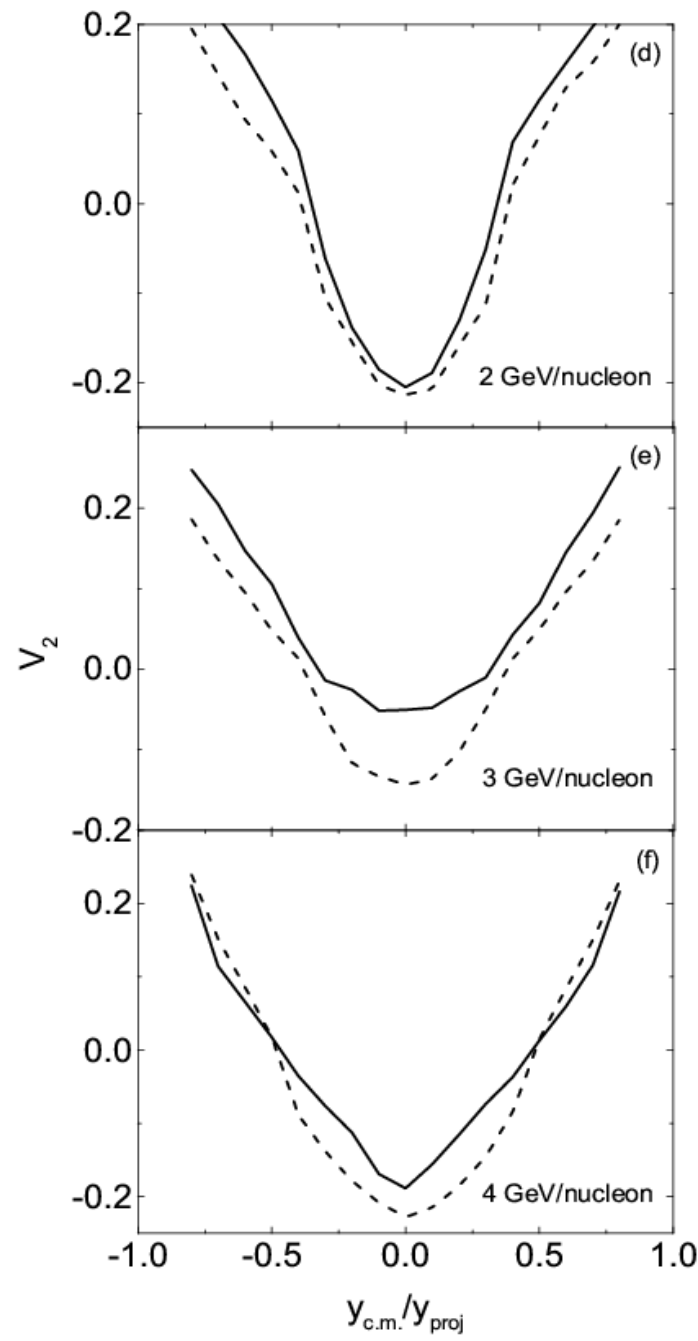
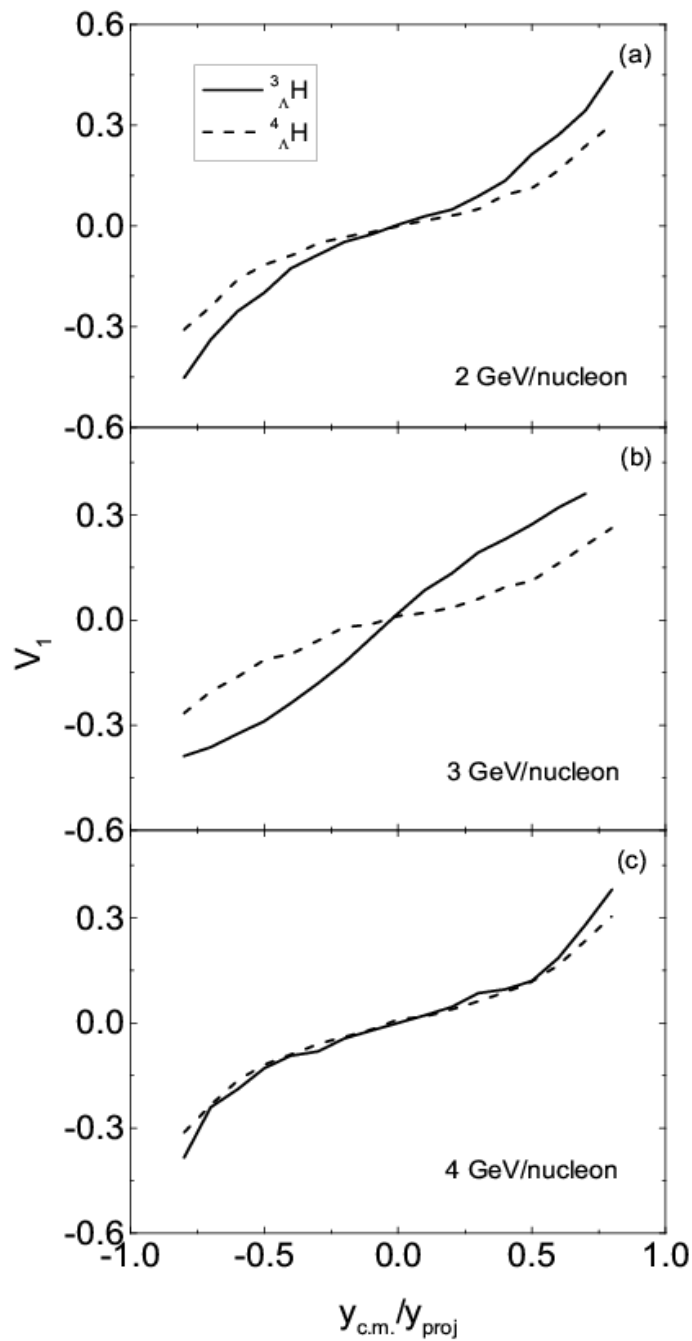
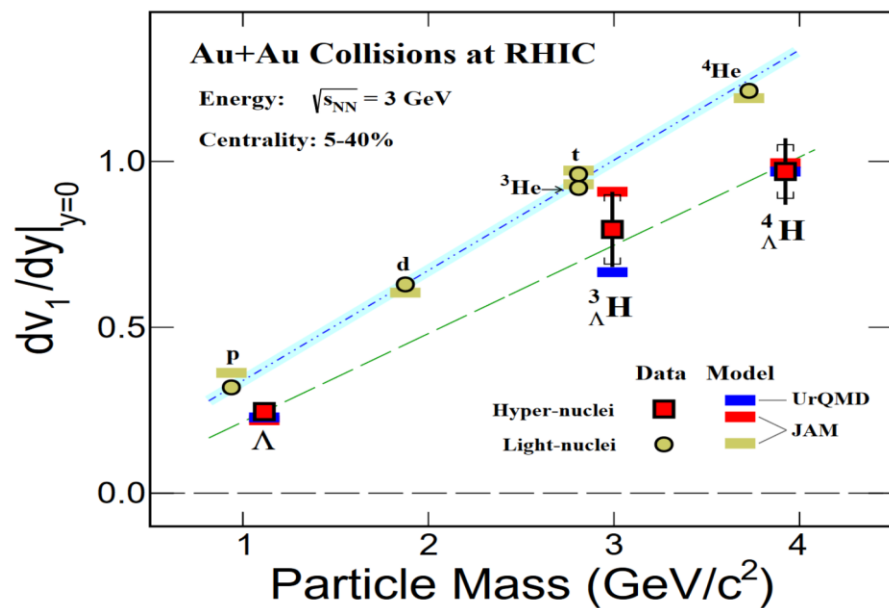
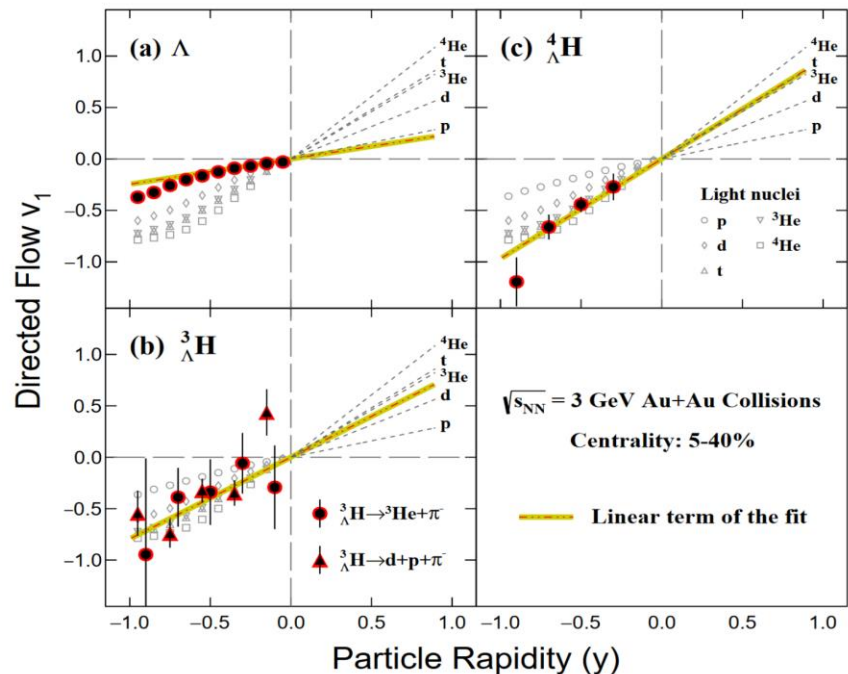
$$\frac{dN_M}{d^3P} = G_M \binom{A}{M} \binom{M}{Z} \frac{1}{A^M} \int \prod_{i=1}^Z f_p(\mathbf{r}_i, \mathbf{p}_i) \prod_{i=Z+1}^M f_n(\mathbf{r}_i, \mathbf{p}_i) \times \rho^W(\mathbf{r}_{k_1}, \mathbf{p}_{k_1}, \dots, \mathbf{r}_{k_{M-1}}, \mathbf{p}_{k_{M-1}}) \delta(\mathbf{P} - (\mathbf{p}_1 + \dots + \mathbf{p}_M)) d\mathbf{r}_1 d\mathbf{p}_1 \dots d\mathbf{r}_M d\mathbf{p}_M$$

${}^3_{\Lambda}\text{H}$ via ${}^{197}\text{Au}+{}^{197}\text{Au}$



Cal: Eur. Phys. J. A, 57 (2021) 18; FOPI data from Nucl. Phys. A 876, 1 (2012)





3) Surface coalescence for cluster construction

A. Boudard, J. Cugnon, S. Leray et al., Nucl. Phys. A 740, 195-210 (2004)

Hui-Gan Cheng, Zhao-Qing Feng, Chinese Physics C 45, 084107 (2021)

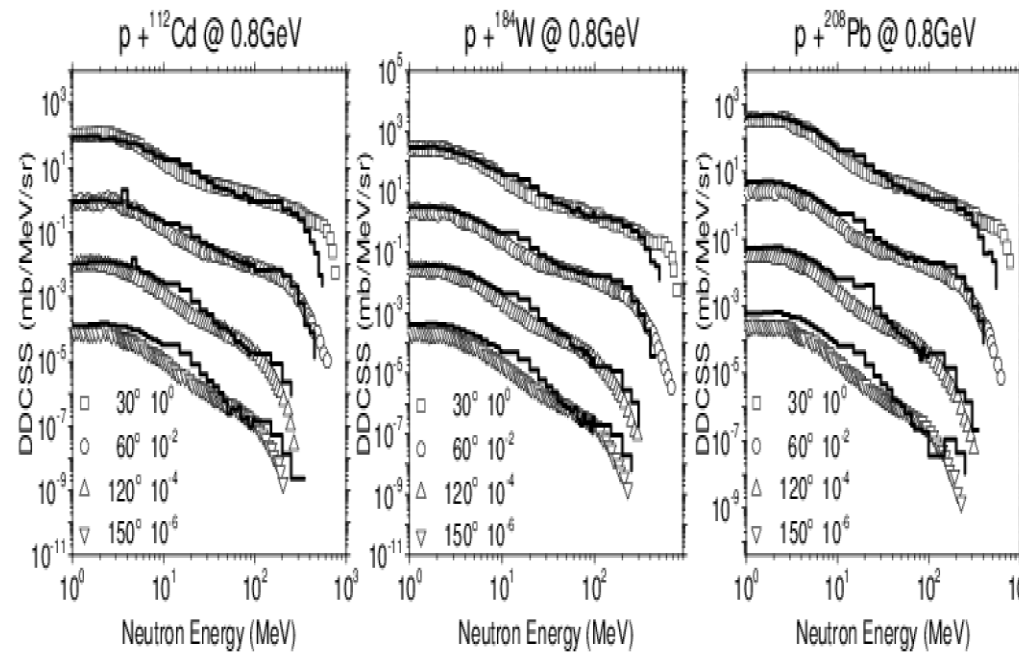
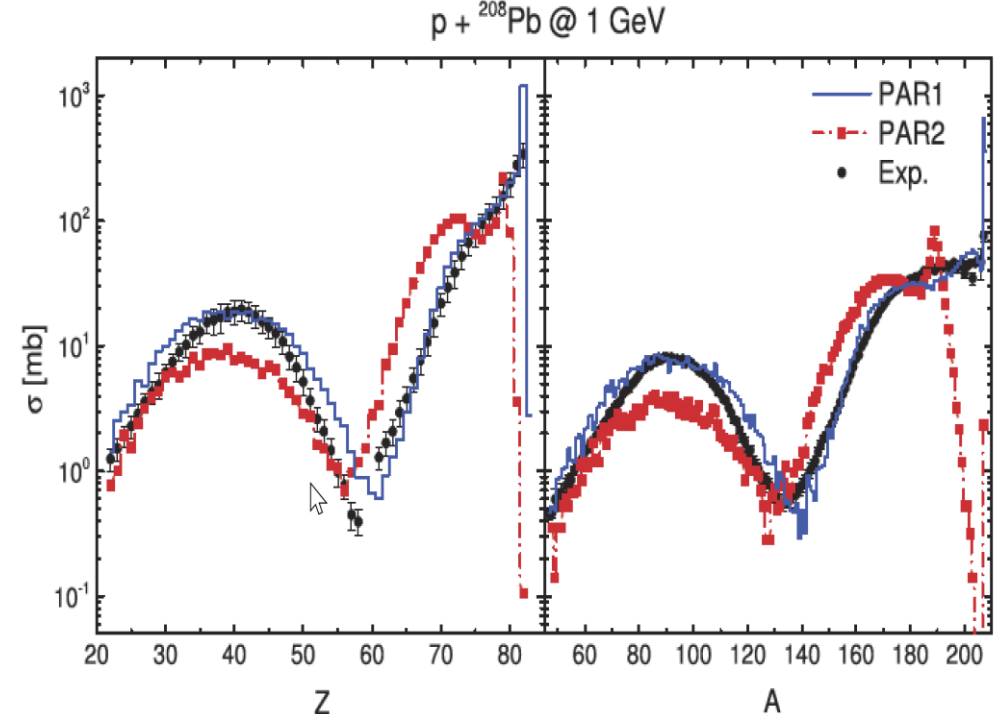
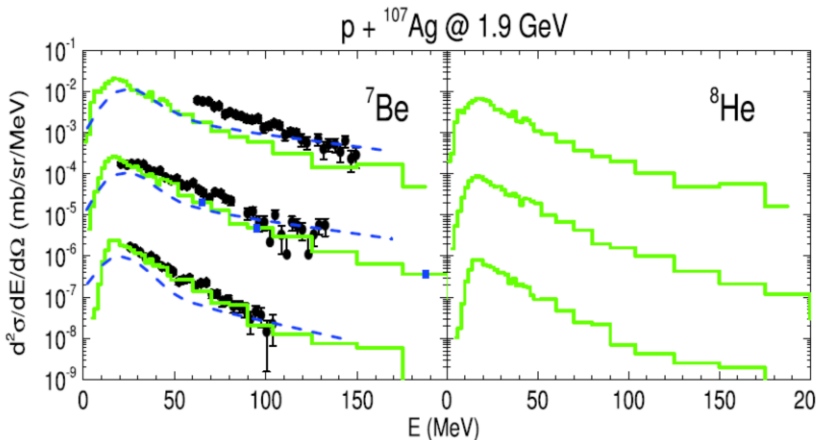
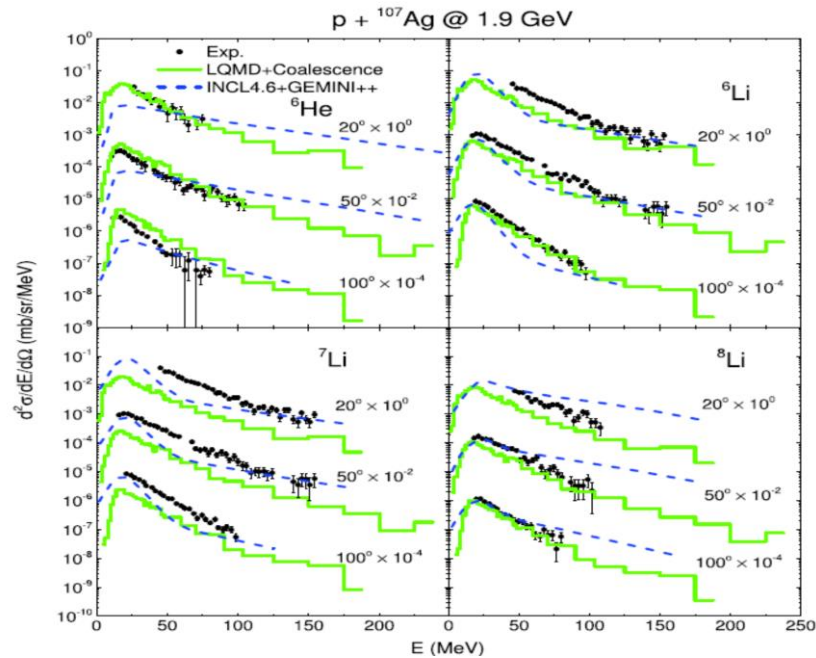
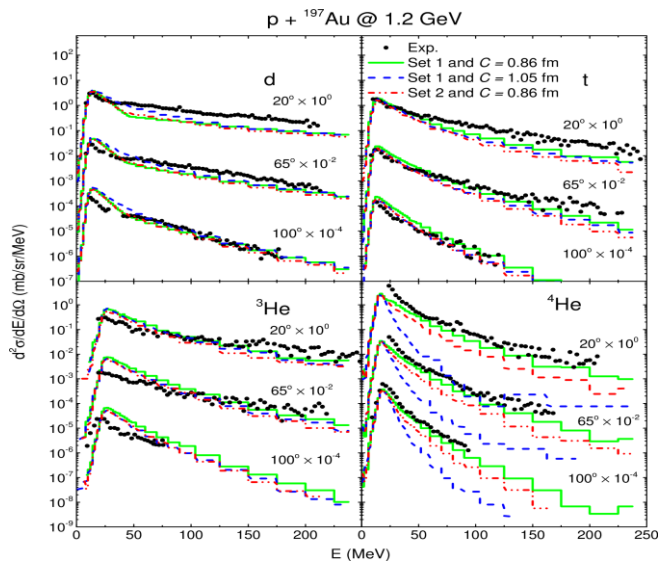
$$R_{Nj} P_{Nj} \leq h_0, \quad R_{Nj} \geq 1 \text{ fm},$$

$$R_{Nj} = |\mathbf{R}_N - \mathbf{r}_j|,$$

$$P_{Nj} = \left| \frac{m_j}{M_N + m_j} \mathbf{p}_N - \frac{M_N}{M_N + m_j} \mathbf{p}_j \right|$$

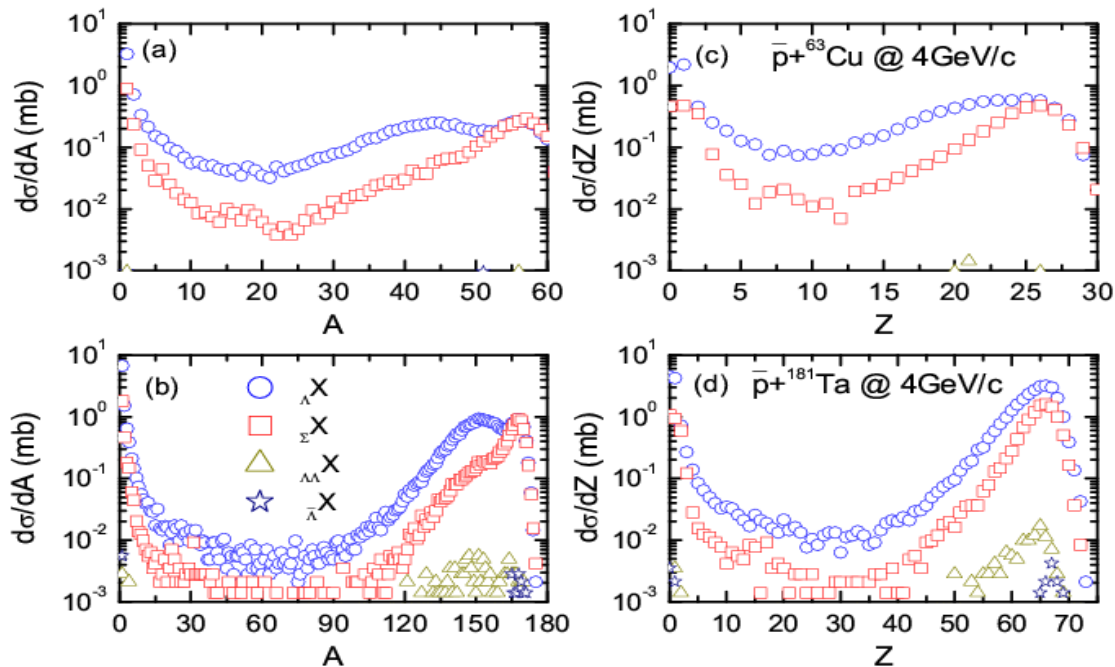
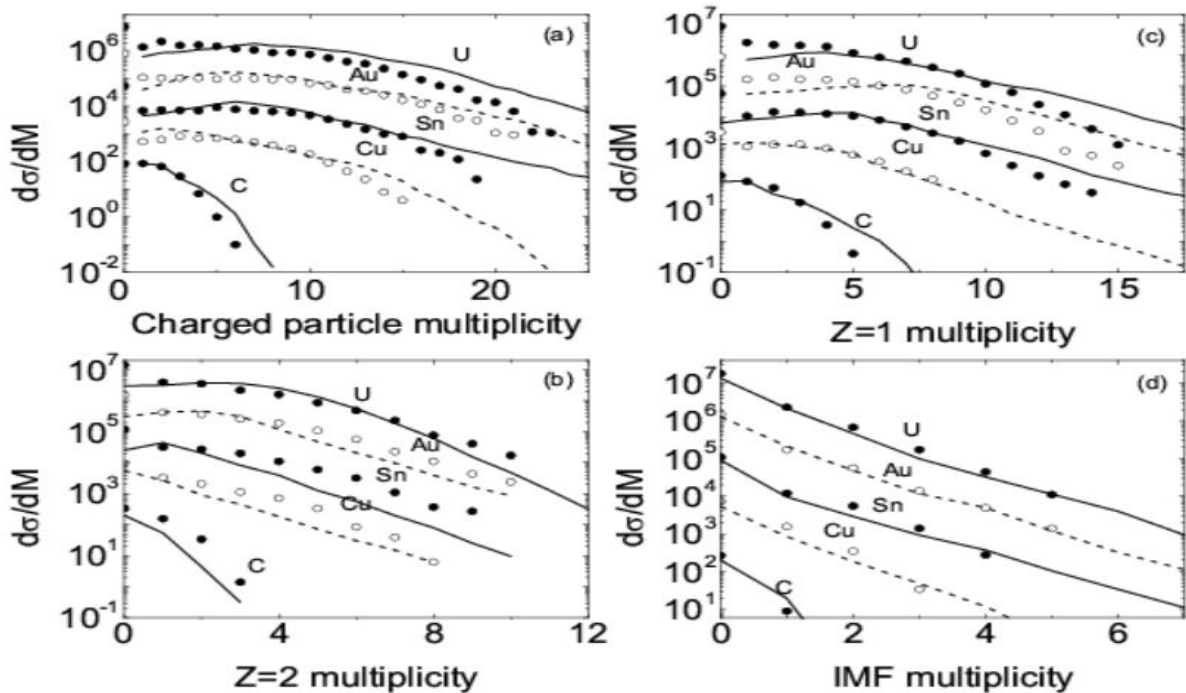
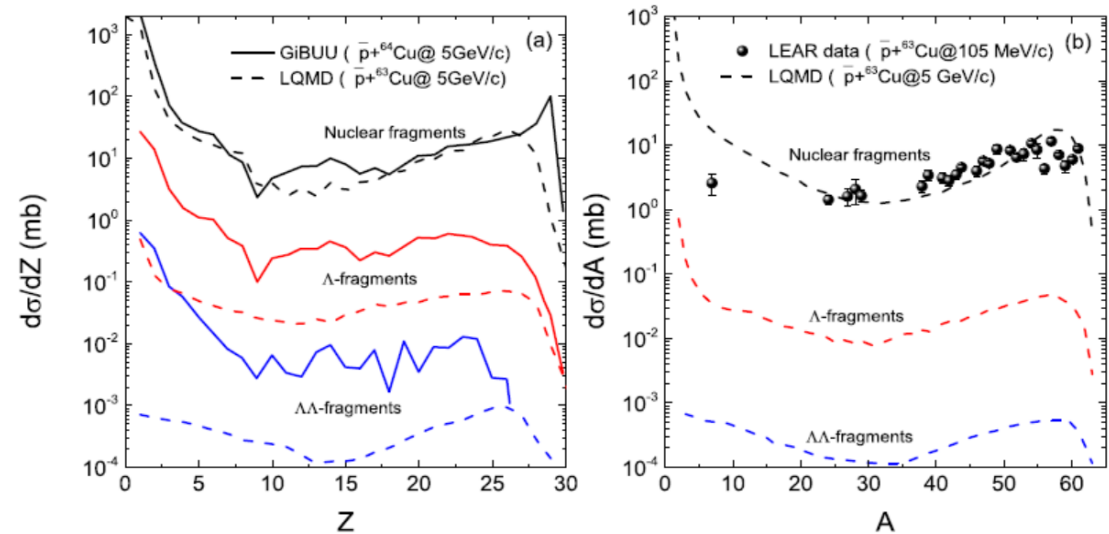
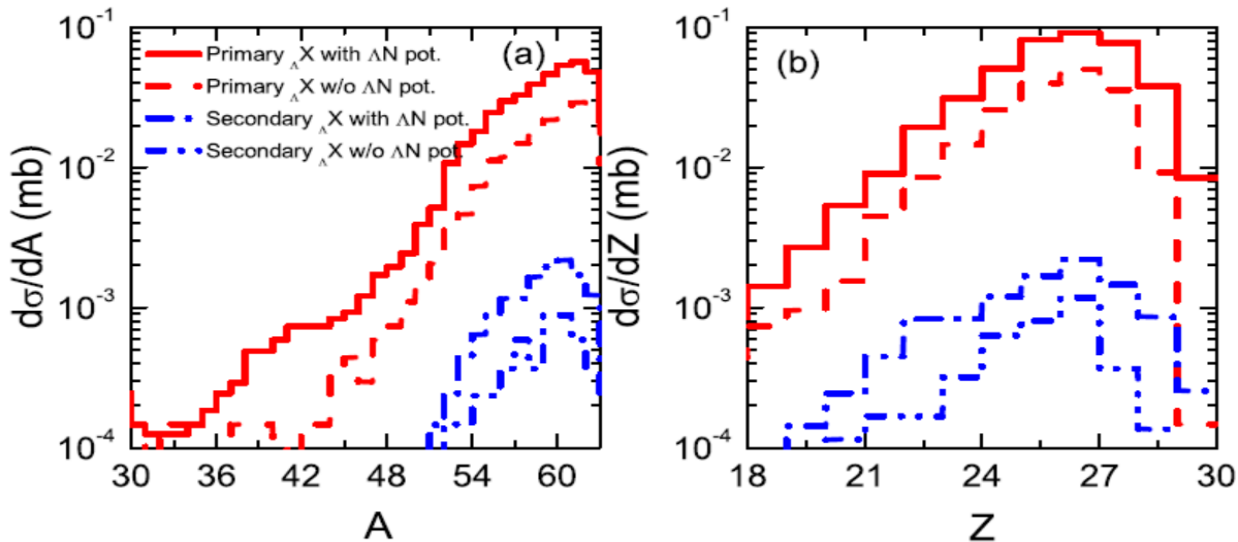
Table 2. Surface coalescence parameters of Set 1 and Set 2.

Construction	$h_0 / (\text{fm MeV}/c)$	
	Set 1	Set 2
$p+n \rightarrow d$	387	336
$d+n \rightarrow t$	387	315
$d+p \rightarrow {}^3\text{He}$	387	315
$t+p \rightarrow {}^4\text{He}$	387	300
${}^3\text{He}+n \rightarrow {}^4\text{He}$	387	300



反质子引起的核反应中核碎片和超核形成

Zhao-Qing Feng, Physical Review C 101, 064601 (2020); 93, 041601(R) (2016)



4) Kinetic approach for cluster production

P. DANIELEWICZ and G. F. BERTSCH, Nuclear Physics A533 (1991) 712-748

Akira Ono, Prog. Part. Nucl. Phys. 105, 139-179 (2019)

R. Wang, Y. G. Ma, L. W. Chen et al., Phys. Rev. C 108, L031601 (2023)

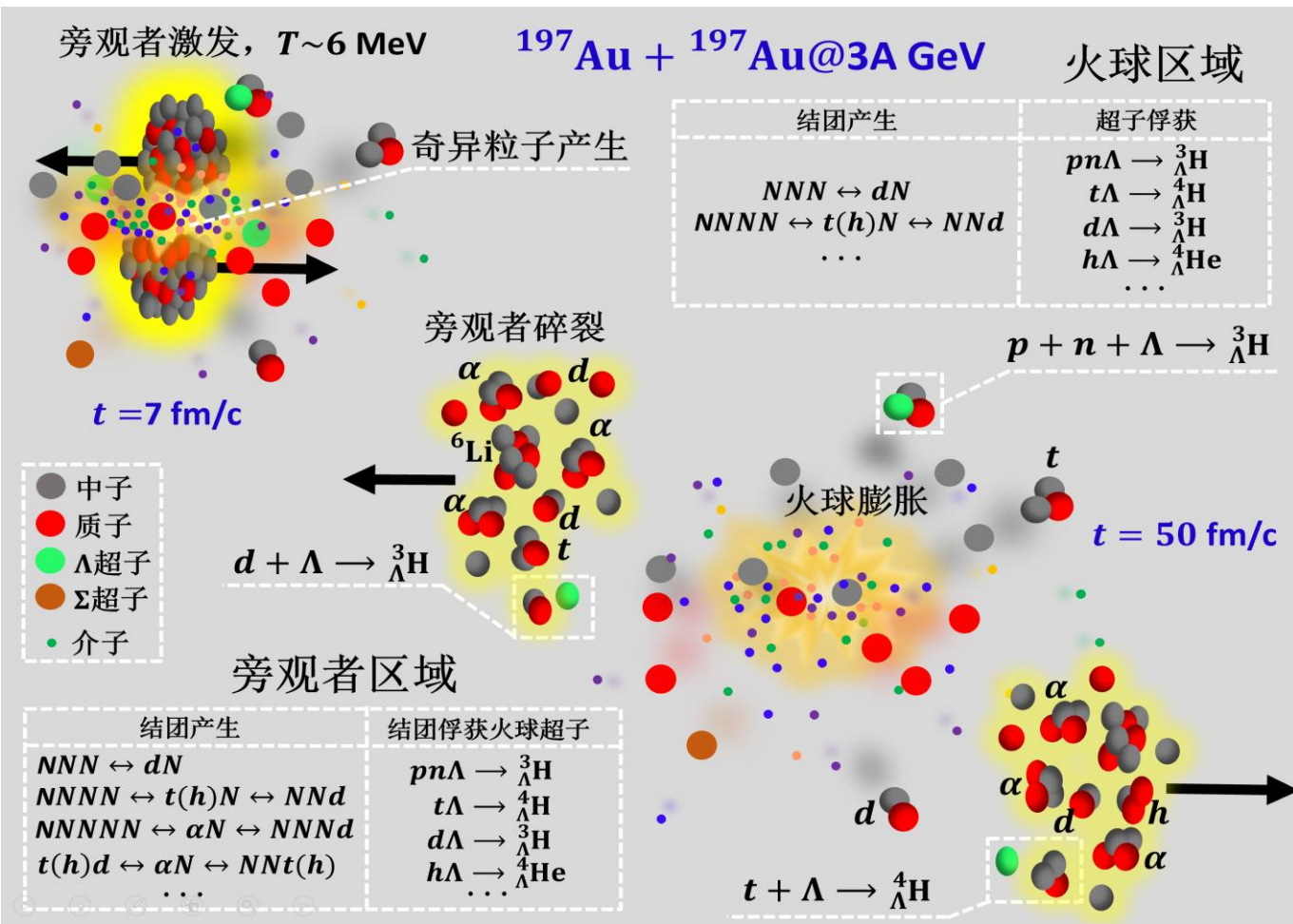
Preequilibrium cluster emission and fragmentation reactions in heavy-ion collisions

Hui-Gan Cheng and Zhao-Qing Feng*

arXiv: 2308.04852

School of Physics and Optoelectronics, South China University of Technology, Guangzhou 510640, China

(Dated: August 10, 2023)

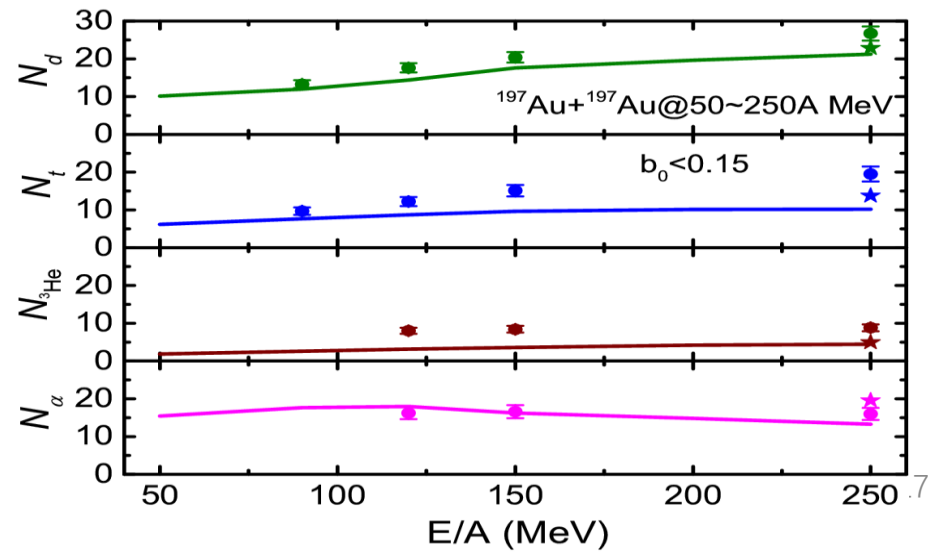
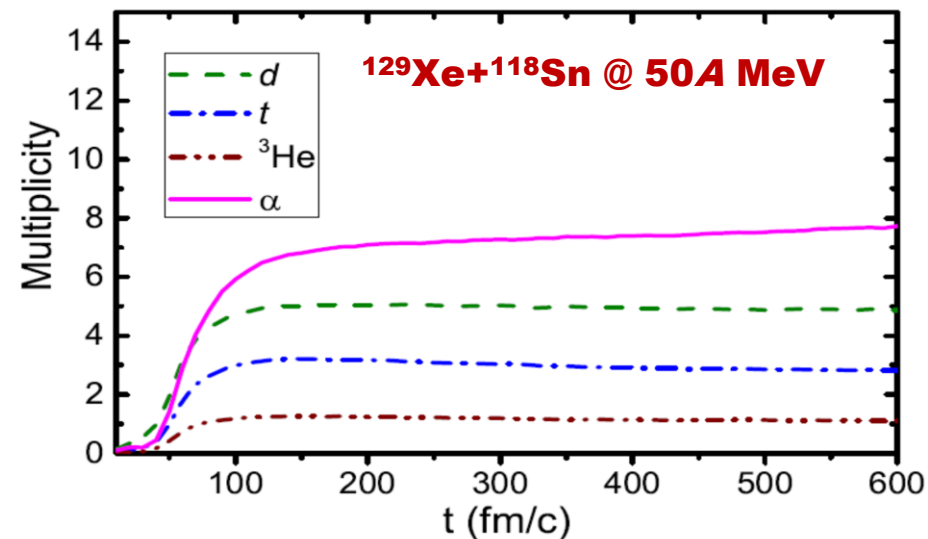


PRODUCTION OF DEUTERONS AND PIONS IN A TRANSPORT MODEL OF ENERGETIC HEAVY-ION REACTIONS

P. DANIELEWICZ and G.F. BERTSCH

National Superconducting Cyclotron Laboratory and Department of Physics and Astronomy,
Michigan State University, East Lansing, MI 48824, USA

Received 8 April 1991
(Revised 21 May 1991)



Transport models for heavy-ion collisions

Progress in Particle and Nuclear Physics 125 (2022) 103962

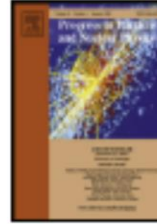


ELSEVIER

Contents lists available at ScienceDirect

Progress in Particle and Nuclear Physics

journal homepage: www.elsevier.com/locate/ppnp



Review

Transport model comparison studies of intermediate-energy heavy-ion collisions

Hermann Wolter^{1,*}, Maria Colonna², Dan Cozma³, Pawel Danielewicz^{4,5}, Che Ming Ko⁶, Rohit Kumar⁴, Akira Ono⁷, ManYee Betty Tsang^{4,5}, Jun Xu^{8,9}, Ying-Xun Zhang^{10,11}, Elena Bratkovskaya^{12,13}, Zhao-Qing Feng¹⁴, Theodoros Gaitanos¹⁵, Arnaud Le Fèvre¹², Natsumi Ikeno¹⁶, Youngman Kim¹⁷, Swagata Mallik¹⁸, Paolo Napolitani¹⁹, Dmytro Oliinychenko²⁰, Tatsuhiko Ogawa²¹, Massimo Papa², Jun Su²², Rui Wang^{9,23}, Yong-Jia Wang²⁴, Janus Weil²⁵, Feng-Shou Zhang^{26,27}, Guo-Qiang Zhang⁹, Zhen Zhang²², Joerg Aichelin²⁸, Wolfgang Cassing²⁵, Lie-Wen Chen²⁹, Hui-Gan Cheng¹⁴, Hannah Elfner^{12,13,20}, K. Gallmeister²⁵, Christoph Hartnack²⁸, Shintaro Hashimoto²¹, Sangyong Jeon³⁰, Kyungil Kim¹⁷, Myungkuk Kim³¹, Bao-An Li³², Chang-Hwan Lee³³, Qing-Feng Li^{24,34}, Zhu-Xia Li¹⁰, Ulrich Mosel²⁵, Yasushi Nara³⁵, Koji Niita³⁶, Akira Ohnishi³⁷, Tatsuhiko Sato²¹, Taesoo Song¹², Agnieszka Sorensen^{38,39}, Ning Wang^{11,40}, Wen-Jie Xie⁴¹, (TMEP collaboration)

Table 1

List of transport models that participated in the TMEP code comparisons discussed in this paper. The columns give the information on the name of the code, the main correspondents of the code, the energy range intended for the code, the treatment of effects of relativity (see Section 2.1), and the comparisons in which the code participated. The different comparisons are listed in the last column in the table by a numbers n , which refer to the subsections 3.n, where they are described in detail: $n = 1$ for Au+Au collisions around 1 AGeV, $n = 2$ for Au+Au collision at 100 and 400 AMeV, $n = 3$ for box-Vlasov, $n = 4$ for box-cascade with only nucleons, $n = 5$ for box-cascade with pion and Δ resonance production, and $n = 6$ for the prediction of pion ratios for Sn+Sn collisions.

BUU Type	Code Correspondents	Energy Range [A GeV]	Relativity	Comparisons
BLOB	P. Napolitani, M. Colonna	0.01–0.5	non-rel	2
BUU-VM	S. Mallik	0.02–1	rel	3,4,5
DJBUU	Y. Kim, S. Jeon, M. Kim, C.-H. Lee, K. Kim	0.05–2	cov	3
GiBUU	J. Weil, T. Gaitanos, K. Gallmeister, U. Mosel	0.05–40	rel/cov	1,2,3,4
IBL	W.J. Xie, F.S. Zhang	0.05–2	rel	2
IBUU	J. Xu, L.W. Chen, B.A. Li	0.05–2	rel	2,3,4,5
LBUU(LHV)	R. Wang, Z. Zhang, L.-W. Chen	0.01–1.5	rel	3
pBUU	P. Danielewicz	0.01–12	rel	1,2,3,4,5,6
PHSD	E. Bratkovskaya, W. Cassing	0.1–200	rel/cov	1,6
RBUU	T. Gaitanos	0.05–2	cov	1,2
RVUU	Z. Zhang, C.M. Ko, T. Song	0.05–2	cov	1,2,3,4,5
SMASH	D. Oliinychenko, H. Elfner, A. Sorensen	0.5–200	cov	3,4,5,6
SMF	M. Colonna, P. Napolitani	0.01–0.5	non-rel	2,3,4
χ BUU	Z. Zhang, C.M. Ko	0.01–0.5	non-rel	6

QMD Type	Code Correspondents	Energy Range [AGeV]	Relativity	Comparisons
AMD	A. Ono	0.01–0.3	non-rel	2
AMD+JAM	N. Ikeno, A. Ono	0.01–0.3	non-rel+rel	6
BQMD/IQMD	A. Le Fèvre, J. Aichelin, C. Hartnack, R. Kumar	0.05–2	rel	1,2,6
CoMD	M. Papa	0.01–0.3	non-rel	2,4
ImQMD	Y.X. Zhang, N. Wang, Z.X. Li	0.02–0.4	rel	2,3,4
IQMD-BNU	J. Su, F.S. Zhang	0.05–2	rel	2,3,4,5,6
IQMD-SINAP	G.Q. Zhang	0.05–2	rel	2
JAM	A. Ono, N. Ikeno, Y. Nara, A. Ohnishi	1–158	rel	4,5
JQMD 2.0	T. Ogawa, K. Niita, S. Hashimoto, T. Sato	0.01–3	rel	4,5
LQMD(IQMD-IMP)	Z.Q. Feng, H.G. Cheng	0.01–10	rel	2,3,4,5
TuQMD/dcQMD	D. Cozma	0.1–2	rel	1,2,3,4,5,6
UrQMD	Y. J. Wang, Q. F. Li, Y. X. Zhang	0.05–200	rel	1,2,3,4,6

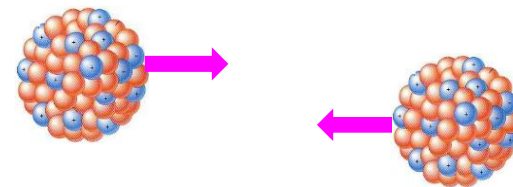
二、LQMD运输模型



重离子运输模型(LQMD)

Heavy-ion collisions (5 MeV – 5 GeV/nucleon) and hadron induced reaction (p , \bar{p} , π , K , e , etc)

- 兰州量子分子动力学模型 (Skyrme interaction, Walecka model with σ , ω , ρ , δ)
- 利用中高能重离子碰撞研究中子星物质状态方程 (nuclear **symmetry energy** at sub- and supra- saturation densities in HICs, isospin splitting of nucleon effective mass from HICs, particle production, 2-body and 3-body potential, multi-body correlation)
- 中高能重离子强子核介质效应研究 (optical potentials, energy conservation and in-medium effects, i.e., $\Delta(1232)$, $N^*(1440)$, $N^*(1535)$), hyperons (Λ, Σ, Ξ) and mesons ($\pi, K, \eta, \rho, \omega, \phi \dots$)
- 核结团和超核结团产生动力学 (production cross section, phase-space distribution, collective flows, cluster transportation, Mott effect, e.g., deuteron, triton, ^3He , α , ${}_{\Lambda(\Sigma)}\text{X}$, ${}_{\Lambda\Lambda}\text{X}$, ${}_{\Xi}\text{X}$, ${}_{\bar{\Lambda}}\text{X}$)



量子分子动力学输运模型

1. 基于Skyrme相互作用的量子分子动力学模型 (LQMD-Skyrme)

PHYSICAL REVIEW C 84, 024610 (2011)

$$H_B = \sum_i \sqrt{\mathbf{p}_i^2 + \mathbf{m}_i^2} + U_{\text{int}} + U_{\text{mom}}$$

Momentum dependence of the symmetry potential and its influence on nuclear reactions

Zhao-Qing Feng*

Institute of Modern Physics, Chinese Academy of Sciences, Lanzhou 730000, People's Republic of China

(Received 11 July 2011; published 19 August 2011)

$$U_{\text{loc}} = \int V_{\text{loc}}(\rho(\mathbf{r})) d\mathbf{r}$$

$$V_{\text{loc}}(\rho) = \frac{\alpha}{2} \frac{\rho^2}{\rho_0} + \frac{\beta}{1+\gamma} \frac{\rho^{1+\gamma}}{\rho_0^\gamma} + E_{\text{sym}}^{\text{loc}}(\rho) \rho \delta^2 + \frac{g_{\text{sur}}}{2\rho_0} (\nabla \rho)^2 + \frac{g_{\text{sur}}^{\text{iso}}}{2\rho_0} [\nabla(\rho_n - \rho_p)]^2,$$

$$U_{\text{mom}} = \frac{1}{2\rho_0} \sum_{i,j,j \neq i} \sum_{\tau,\tau'} C_{\tau,\tau'} \delta_{\tau,\tau_i} \delta_{\tau',\tau_j} \iiint d\mathbf{p} d\mathbf{p}' d\mathbf{r} f_i(\mathbf{r}, \mathbf{p}, t) \times [\ln(\epsilon(\mathbf{p} - \mathbf{p}')^2 + 1)]^2 f_j(\mathbf{r}, \mathbf{p}', t).$$

Table 1: The parameters and properties of isospin symmetric EoS used in the LQMD model at the density of 0.16 fm^{-3} .

Parameters	α (MeV)	β (MeV)	γ	C_{mom} (MeV)	ϵ (c^2/MeV^2)	m_∞^*/m	K_∞ (MeV)
PAR1	-215.7	142.4	1.322	1.76	5×10^{-4}	0.75	230
PAR2	-226.5	173.7	1.309	0.	0.	1.	230

$$E_{\text{sym}}(\rho) = \frac{1}{3} \frac{\hbar^2}{2m} \left(\frac{3}{2} \pi^2 \rho \right)^{2/3} + E_{\text{sym}}^{\text{loc}}(\rho) + E_{\text{sym}}^{\text{mom}}(\rho).$$

$$E_{\text{sym}}^{\text{loc}}(\rho) = \frac{1}{2} C_{\text{sym}} (\rho/\rho_0)^{\gamma_s}$$

$$E_{\text{sym}}^{\text{loc}}(\rho) = a_{\text{sym}} (\rho/\rho_0) + b_{\text{sym}} (\rho/\rho_0)^2.$$

$$\begin{aligned} C_{\text{sym}} &= 38 \text{ MeV} \\ a_{\text{sym}} &= 37.7 \text{ MeV} \\ b_{\text{sym}} &= -18.7 \text{ MeV} \end{aligned}$$

2. 相对论量子分子动力学(LQMD-RMF)

$$L = \bar{\psi} [i\gamma_\mu \partial^\mu - (M_N - g_\sigma \varphi - g_\delta \vec{\tau} \cdot \vec{\delta}) - g_\omega \gamma_\mu \omega^\mu - g_\rho \gamma_\mu \vec{\tau} \cdot \vec{b}^\mu] \psi \\ + \frac{1}{2} (\partial_\mu \varphi \partial^\mu \varphi - m_\sigma^2 \varphi^2) - U(\varphi) + \frac{1}{2} (\partial_\mu \vec{\delta} \partial^\mu \vec{\delta} - m_\delta^2 \vec{\delta}^2) \\ + \frac{1}{2} m_\omega^2 \omega_\mu \omega^\mu - \frac{1}{4} F_{\mu\nu} F^{\mu\nu} + \frac{1}{2} m_\rho^2 \vec{b}_\mu \vec{b}^\mu - \frac{1}{4} \vec{G}_{\mu\nu} \vec{G}^{\mu\nu}$$

$$F_{\mu\nu} = \partial_\mu \omega_\nu - \partial_\nu \omega_\mu, \\ G_{\mu\nu} = \partial_\mu \vec{b}_\nu - \partial_\nu \vec{b}_\mu, \\ U(\varphi) = \frac{g_2}{3} \varphi^3 + \frac{g_3}{4} \varphi^4$$

能量密度:

$$\varepsilon = \sum_{i=n,p} 2 \int \frac{d^3k}{(2\pi)^3} \sqrt{k^2 + M_i^{*2}} + \frac{1}{2} m_\sigma^2 \varphi^2 + U(\varphi) + \frac{1}{2} m_\omega^2 \omega_0^2 + \frac{1}{2} m_\rho^2 b_0^2 + \frac{1}{2} m_\delta^2 \delta_3^2$$

核子的相空间演化:

$$\dot{\mathbf{x}} = \frac{\mathbf{p}_i^*}{p_0^*} + \sum_{i \neq j}^N \left\{ \frac{g_v^2}{2m_v^2} z_j^{*\mu} u_{i,\mu} B_i B_j \frac{\partial \rho_{ij}}{\partial \mathbf{p}_i} + \frac{g_v^2}{2m_v^2} z_i^{*\mu} u_{j,\mu} B_i B_j \frac{\partial \rho_{ji}}{\partial \mathbf{p}_i} + \frac{g_v^2}{2m_v^2} z_j^{*\mu} \rho_{ji} B_i B_j \frac{\partial u_{i,\mu}}{\partial \mathbf{p}_i} \right. \\ \left. + z_j^{*\mu} \frac{B_i B_j \bar{g}_v^2}{2m_v^2} \left[\frac{\rho_{ij}}{1 - p_{T,ij}^2/\Lambda_v^2} \frac{\partial u_{i,\mu}}{\partial \mathbf{p}_i} + \frac{u_{i,\mu}}{1 - p_{T,ij}^2/\Lambda_v^2} \frac{\partial \rho_{ij}}{\partial \mathbf{p}_i} + u_{i,\mu} \rho_{ij} \frac{\partial [1/(1 - p_{T,ij}^2/\Lambda_v^2)]}{\partial \mathbf{p}_i} \right] \right. \\ \left. + z_i^{*\mu} \frac{B_i B_j \bar{g}_v^2}{2m_v^2} \left[\frac{u_{j,\mu}}{1 - p_{T,ji}^2/\Lambda_v^2} \frac{\partial \rho_{ji}}{\partial \mathbf{p}_i} + u_{j,\mu} \rho_{ji} \frac{\partial [1/(1 - p_{T,ji}^2/\Lambda_v^2)]}{\partial \mathbf{p}_i} \right] \right. \\ \left. - \frac{m_j^*}{p_j^{*0}} \frac{\partial S_j}{\partial \mathbf{p}_i} - \frac{m_i^*}{p_i^{*0}} \frac{\partial S_i}{\partial \mathbf{p}_i} \right\},$$

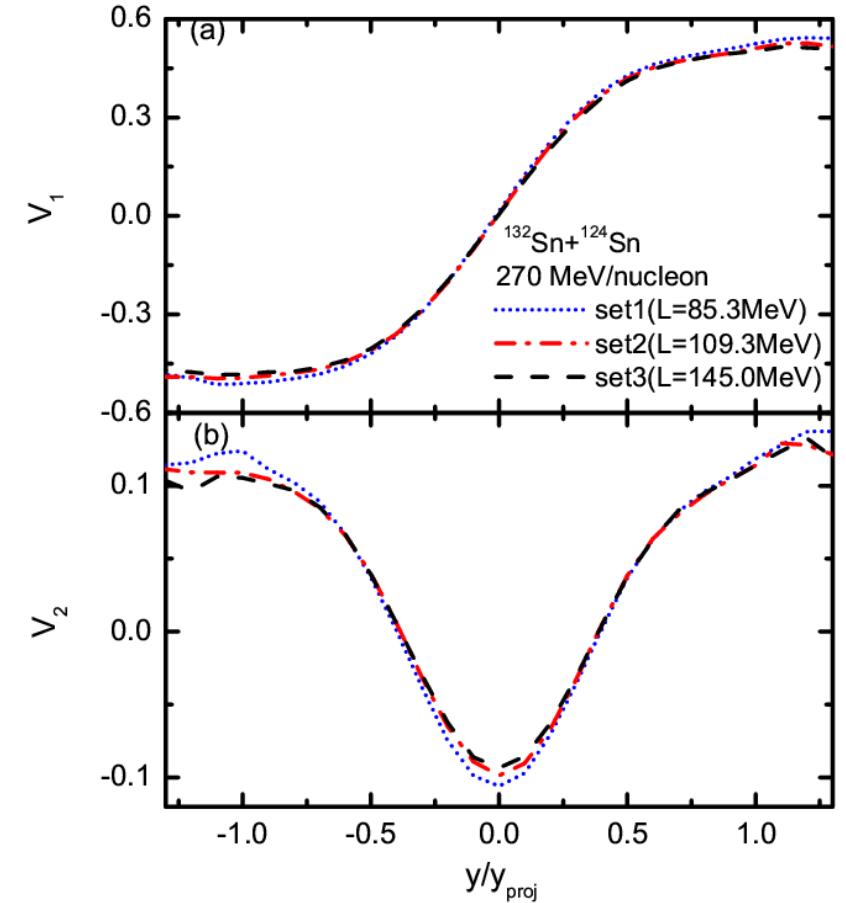
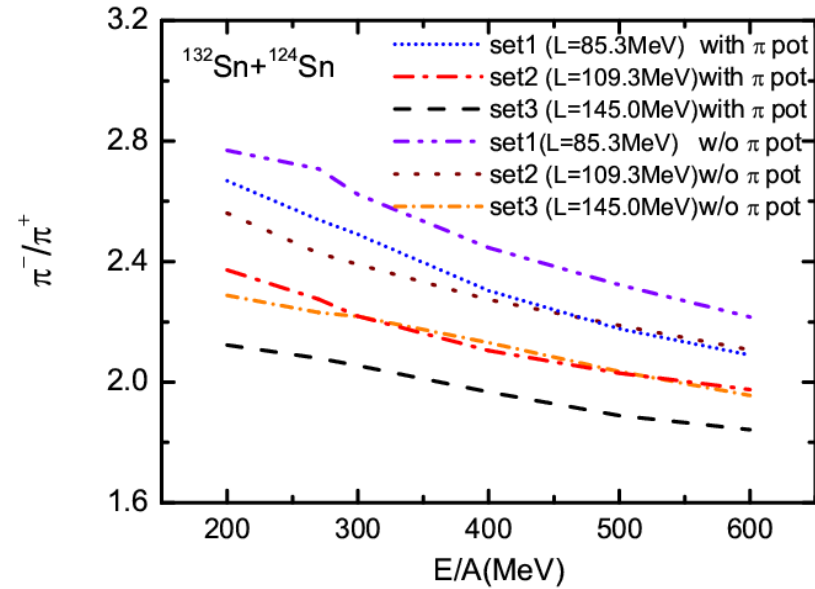
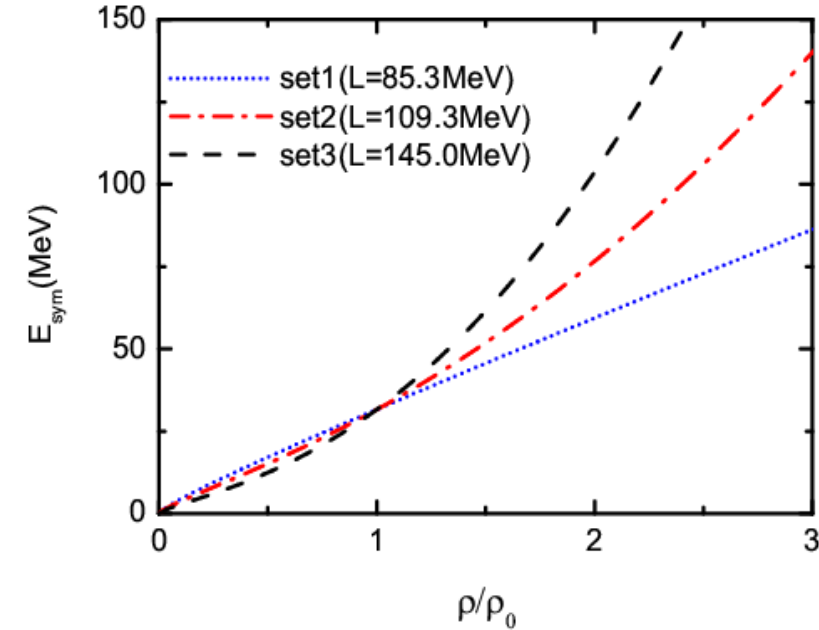
$$\dot{\mathbf{p}} = - \sum_{i \neq j}^N \left\{ \frac{g_v^2}{2m_v^2} z_j^{*\mu} u_{i,\mu} B_i B_j \frac{\partial \rho_{ij}}{\partial \mathbf{r}_i} + \frac{g_v^2}{2m_v^2} z_i^{*\mu} u_{j,\mu} B_i B_j \frac{\partial \rho_{ji}}{\partial \mathbf{r}_i} \right. \\ \left. + z_j^{*\mu} \frac{B_i B_j \bar{g}_v^2}{2m_v^2} \frac{u_{i,\mu}}{1 - p_{T,ij}^2/\Lambda_v^2} \frac{\partial \rho_{ij}}{\partial \mathbf{r}_i} \right. \\ \left. + z_i^{*\mu} \frac{B_i B_j \bar{g}_v^2}{2m_v^2} \frac{u_{j,\mu}}{1 - p_{T,ji}^2/\Lambda_v^2} \frac{\partial \rho_{ji}}{\partial \mathbf{r}_i} \right. \\ \left. - \frac{m_j^*}{p_j^{*0}} \frac{\partial S_j}{\partial \mathbf{r}_i} - \frac{m_i^*}{p_i^{*0}} \frac{\partial S_i}{\partial \mathbf{r}_i} \right\},$$

TABLE I: Parameter sets for RMF. The saturation density ρ_0 is set to be 0.16 fm^{-3} . The binding energy of saturation density is $E/A - M_N = -16 \text{ MeV}$. The isoscalar-vector ω and isovector-vector ρ masses are fixed to their physical values, $m_\omega = 783 \text{ MeV}$ and $m_\rho = 763 \text{ MeV}$. The remaining meson mass m_σ is set to be 550 MeV .

model	g_σ	g_ω	$g_2 \text{ (fm}^{-1}\text{)}$	g_3	g_ρ	g_δ	$K \text{ (MeV)}$	$E_{sym}(\rho_0) \text{ (MeV)}$	$L(\rho_0) \text{ (MeV)}$
set1	8.145	7.570	31.820	28.100	4.049	-	230	31.6	85.3
set2	8.145	7.570	31.820	28.100	8.673	5.347	230	31.6	109.3
set3	8.145	7.570	31.820	28.100	11.768	7.752	230	31.6	145.0

核物质对称能
$$E_{sym} = \frac{1}{6} \frac{k_F^2}{E_F^*} + \frac{1}{2} \left[f_\rho - f_\delta \left(\frac{M^*}{E_F^*} \right) \right] \rho$$

$$f_{\rho,\delta} = g_{\rho,\delta} / m_{\rho,\delta}$$



3. 粒子产生反应道

π and resonances ($\Delta(1232)$, $N^*(1440)$, $N^*(1535)$, ...) production:

$$\begin{aligned}
 NN &\leftrightarrow N\Delta, & NN &\leftrightarrow NN^*, & NN &\leftrightarrow \Delta\Delta, & \Delta &\leftrightarrow N\pi, \\
 N^* &\leftrightarrow N\pi, & NN &\leftrightarrow NN\pi(s\text{-state}), & N^*(1535) &\leftrightarrow N\eta
 \end{aligned}$$

Collisions between resonances, $NN^* \leftrightarrow N\Delta$, $NN^* \leftrightarrow NN^*$

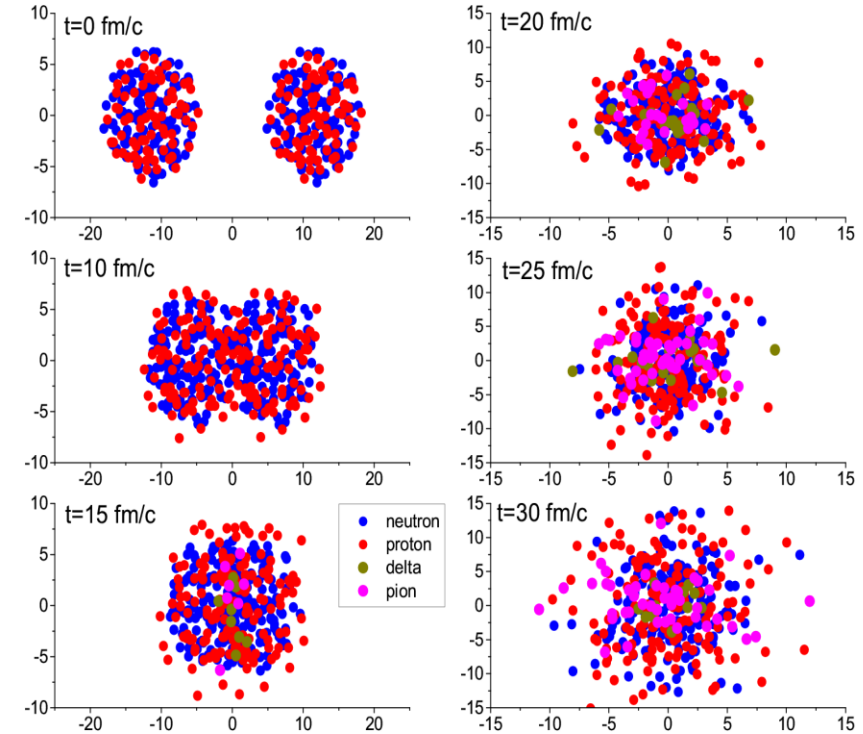
Strangeness channels:

$$\begin{aligned}
 BB &\rightarrow BYK, & BB &\rightarrow BBK\bar{K}, & B\pi(\eta) &\rightarrow YK, & YK &\rightarrow B\pi, \\
 B\pi &\rightarrow NK\bar{K}, & Y\pi &\rightarrow B\bar{K}, & B\bar{K} &\rightarrow Y\pi, & YN &\rightarrow \bar{K}NN, \\
 BB &\rightarrow B\Xi KK, & \bar{K}B &\leftrightarrow K\Xi, & YY &\leftrightarrow N\Xi, & \bar{K}Y &\leftrightarrow \pi\Xi.
 \end{aligned}$$

Reaction channels with antiproton:

$$\bar{p}N \rightarrow \bar{N}N, \quad \bar{N}N \rightarrow \bar{N}N, \quad \bar{N}N \rightarrow \bar{B}B, \quad \bar{N}N \rightarrow \bar{Y}Y$$

$$\bar{N}N \rightarrow \text{annihilation}(\pi, \eta, \rho, \omega, K, \bar{K}, K^*, \bar{K}^*, \phi)$$



Statistical model with SU(3)

symmetry for annihilation

(E.S. Golubeva et al., Nucl. Phys. A 537, 393 (1992))

The **PYTHIA** and **FRITIOF** code are used for baryon(meson)-baryon and antibaryon-baryon collisions at high invariant energies

4. 超子-核子相互作用

$$V_{opt}^{\Sigma}(\mathbf{p}_i, \rho_i) = V_0(\rho_i/\rho_0)^{\gamma_s} + V_1(\rho_n - \rho_p)t_{\Sigma}\rho_i^{\gamma_s-1}/\rho_0^{\gamma_s} + C_{mom}\rho_i \ln(\epsilon p_i^2 + 1)$$

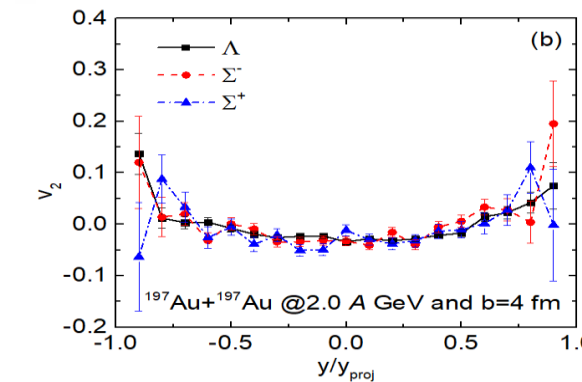
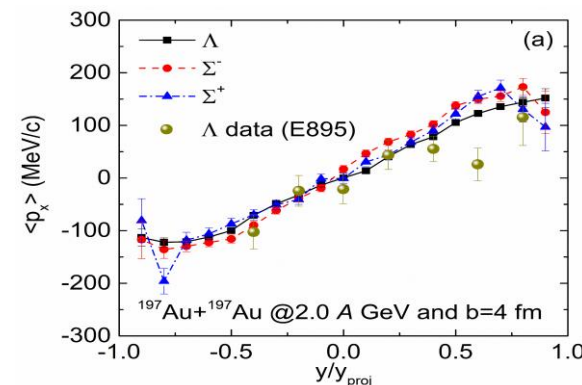
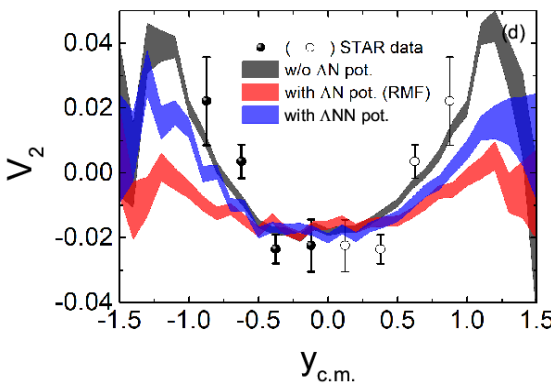
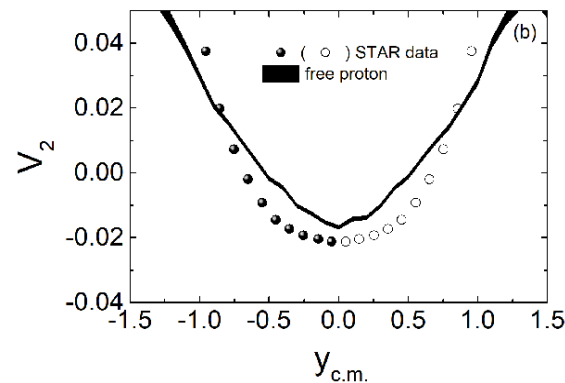
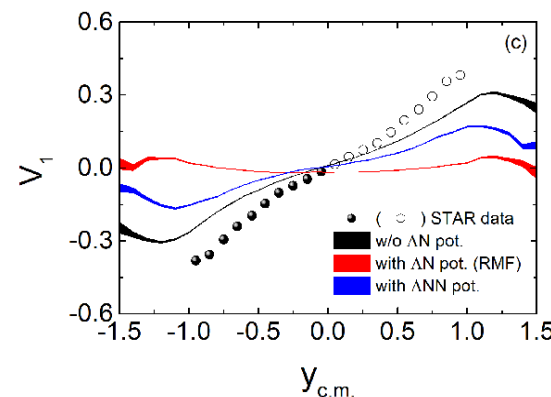
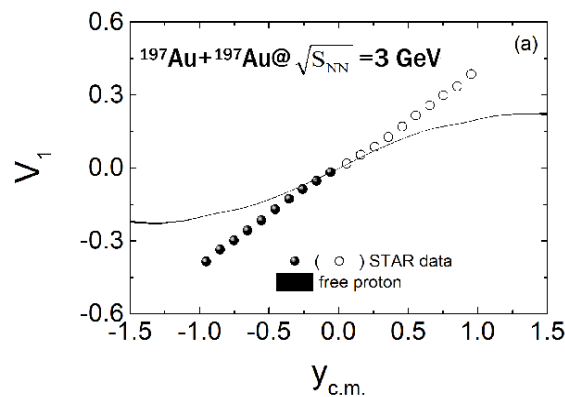
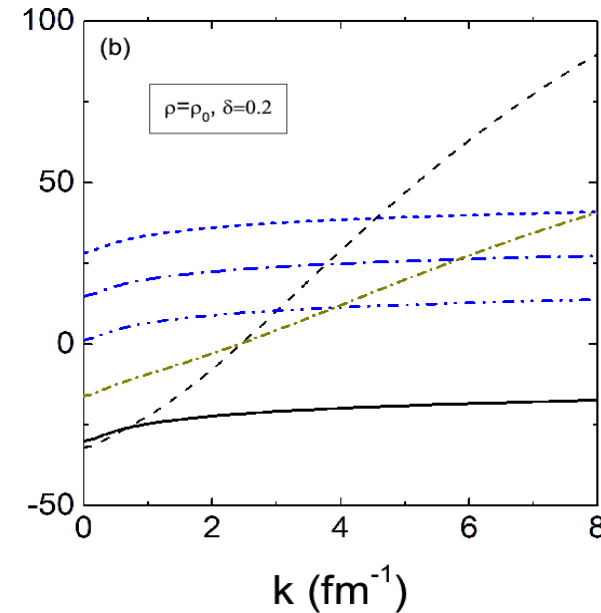
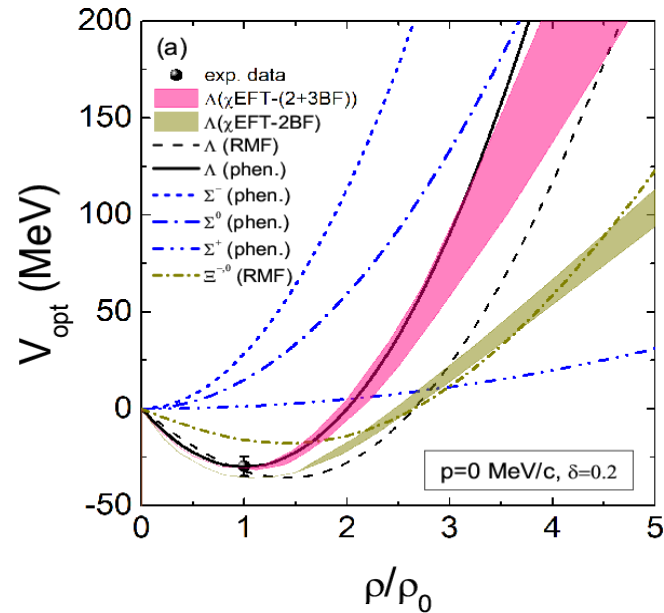
$$V_{opt}^{\Lambda NN}(\mathbf{p}_i, \rho_i) = V_a(\rho_i/\rho_0) + V_b(\rho_i/\rho_0)^2 + C_{mom}(\rho_i/\rho_0) \ln(\epsilon p_i^2 + 1)$$

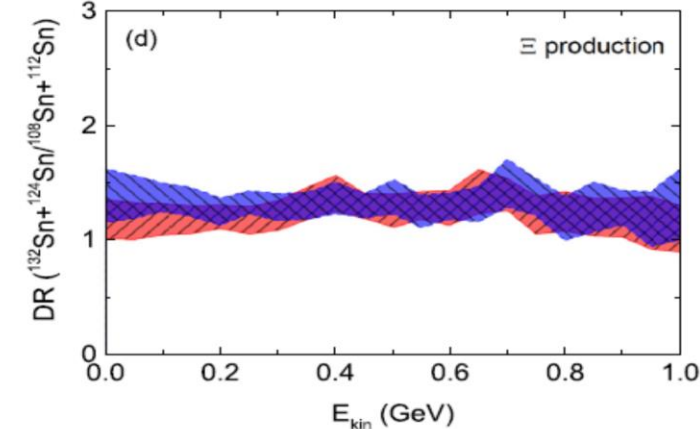
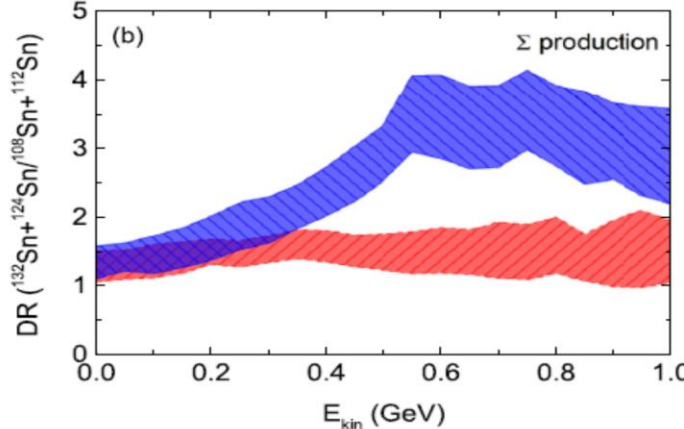
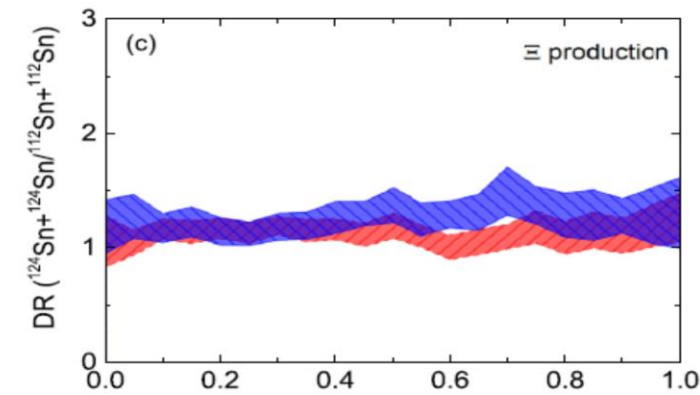
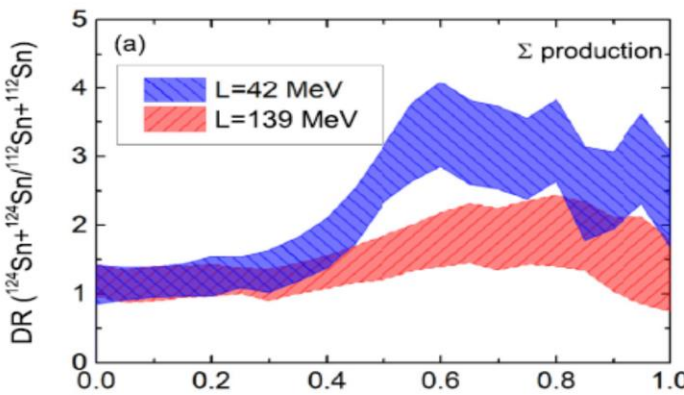
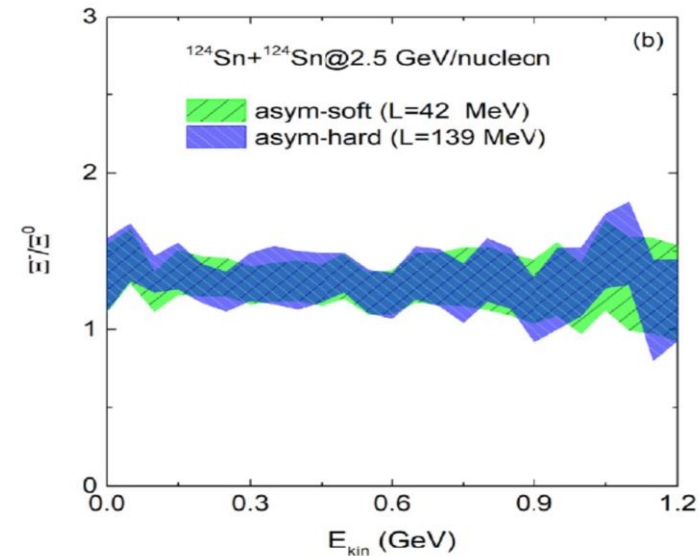
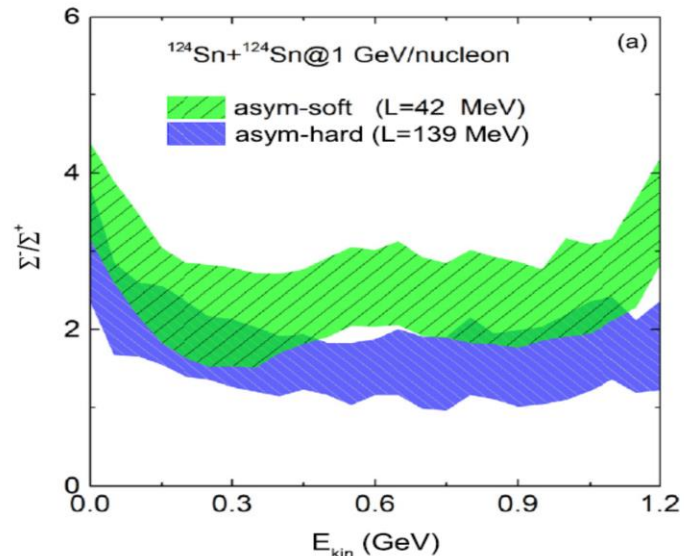
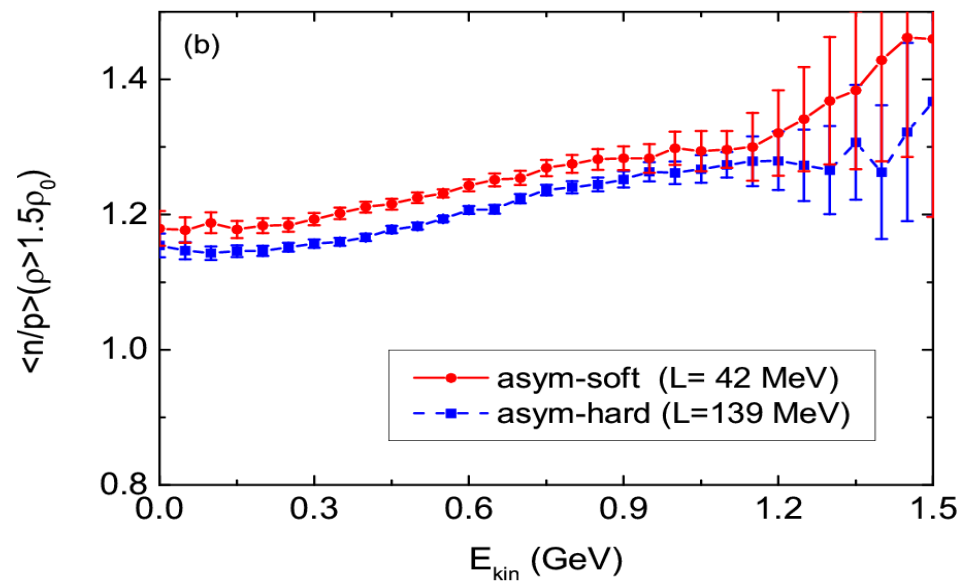
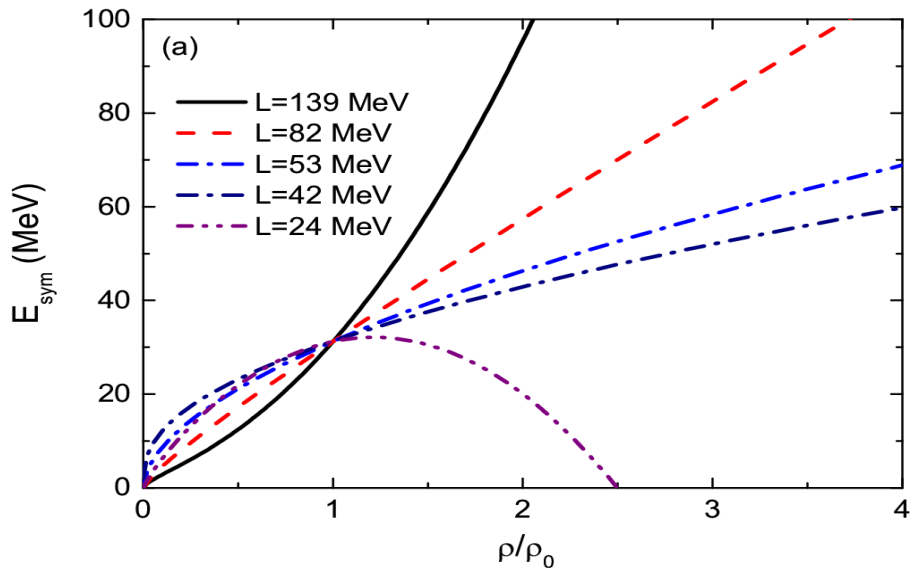
$$V_0 = 14.8 \text{ MeV}, V_1 = 67.8 \text{ MeV},$$

$$V_a = -60 \text{ MeV and } V_b = 30 \text{ MeV}$$

Ding-Chang Zhang, Hui-Gan Cheng and Zhao-Qing Feng, *Chinese Physics Letters* 38 (2021) 092501;

Zhao-Qing Feng, *Physics Letters B* 846, 138180 (2023).





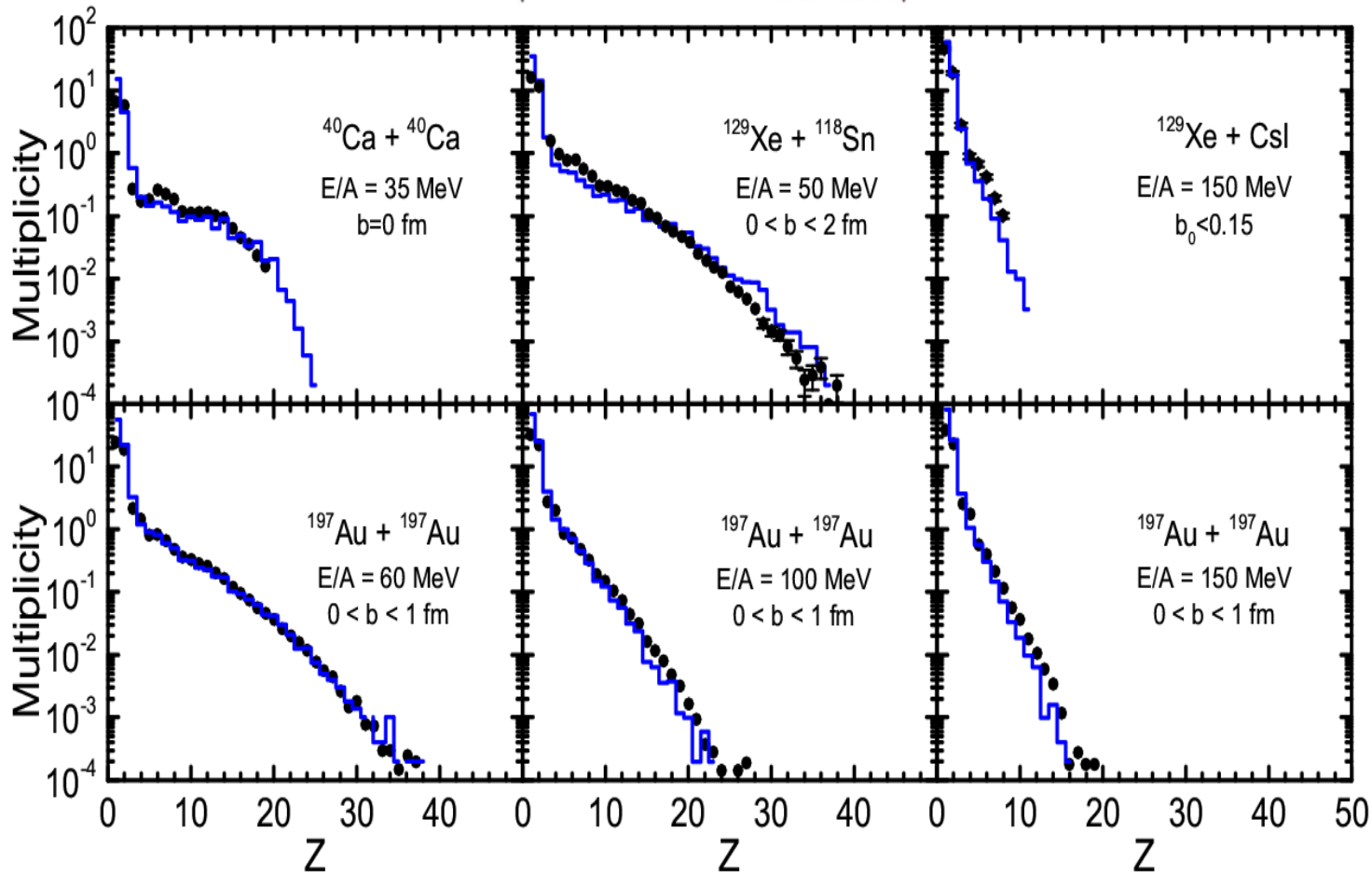
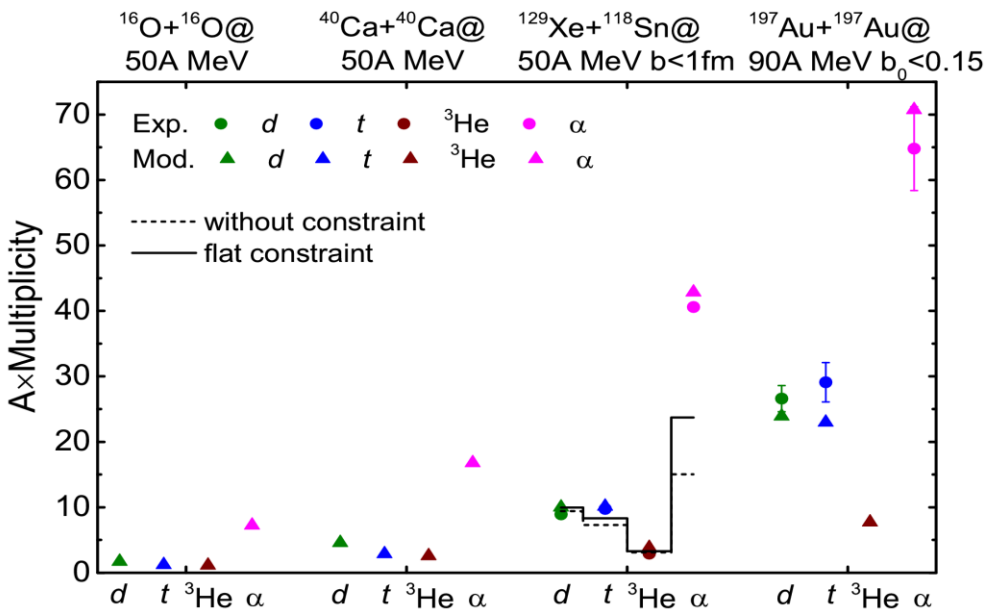
四、重离子碰撞核碎片和超核产生

Hui-Gan Cheng and Zhao-Qing Feng, arXiv: 2308.04852

两体和多体碰撞产生结团和关联

$$\begin{aligned}
 H = & \sum_i \frac{\mathbf{p}_i^2}{2m} + \frac{\alpha}{2} \sum_{i,j} \frac{\rho_{ij}}{\rho_0} + \frac{\beta}{1+\gamma} \sum_i \left(\sum_{j,j \neq i} \frac{\rho_{ij}}{\rho_0} \right)^\gamma \\
 & + \frac{C_{sym}}{2} \sum_{i,j} t_{z_i} t_{z_j} \frac{\rho_{ij}}{\rho_0} + \frac{g_{sur}}{2} \sum'_{i,j} \left[\frac{3}{2L} - \left(\frac{\mathbf{r}_i - \mathbf{r}_j}{2L} \right)^2 \right] \frac{\rho_{ij}}{\rho_0} \\
 & + \sum_i^{N_C} E_{z.p.}^i + \sum_i^{N_d} V_{corr} e^{-r_i^2/4L}
 \end{aligned}$$

$$\frac{d\sigma}{d\Omega} = P(C1 + C2 \rightarrow C3 + C4) \times \frac{v_{\tilde{p}_{rel}}}{v} \frac{|\partial e(k)/\partial k|_{k=\tilde{p}_{rel}}}{|\partial H(p_f)/\partial p_f|_{p_f=p_{rel}}} \frac{p_{rel}^2}{\tilde{p}_{rel}^2} \left[\frac{d\sigma_{NN}}{d\Omega} \right]_{\tilde{p}_{rel}}$$



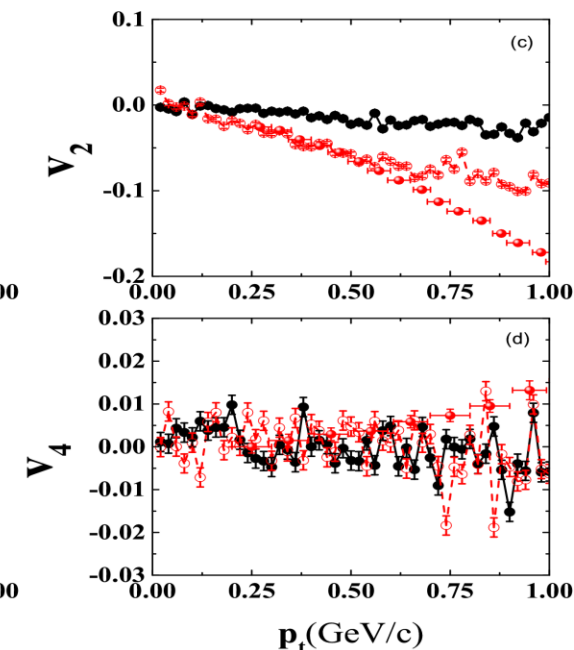
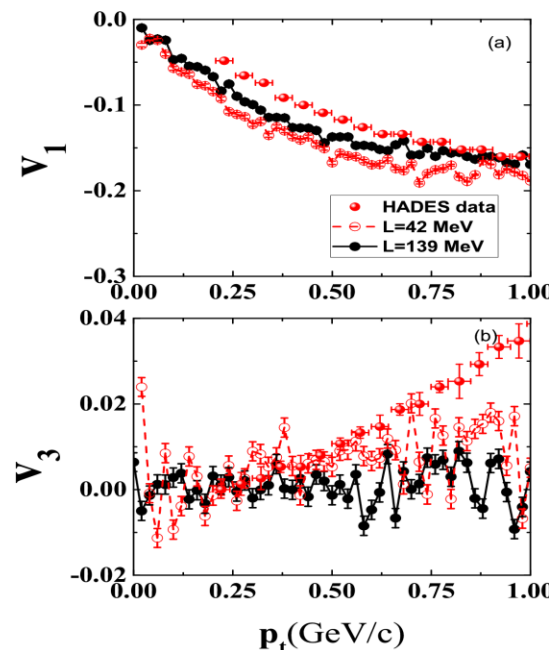
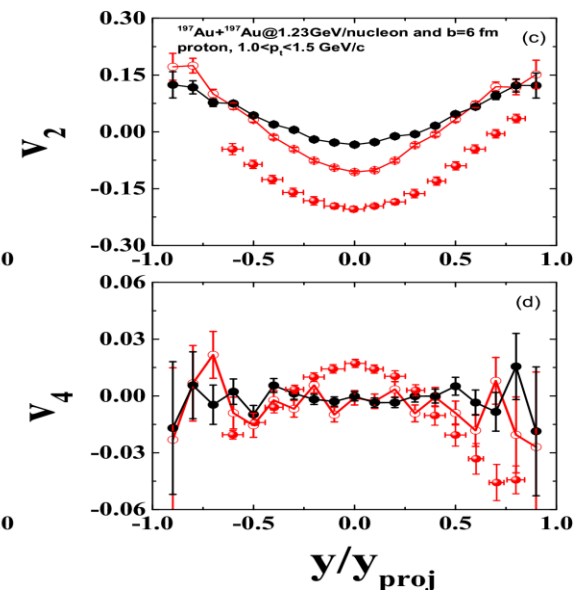
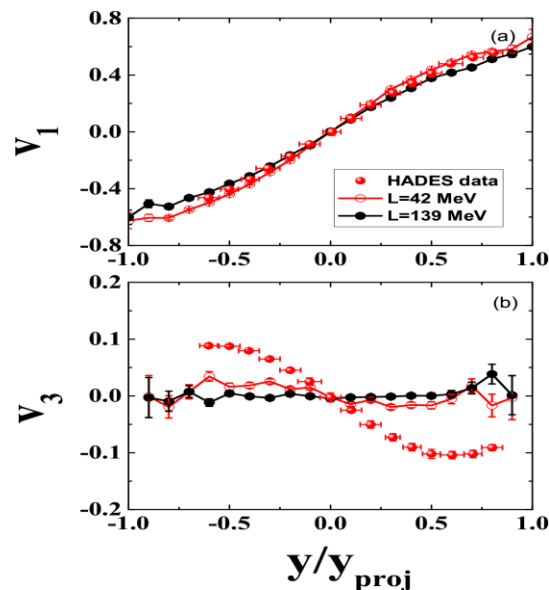
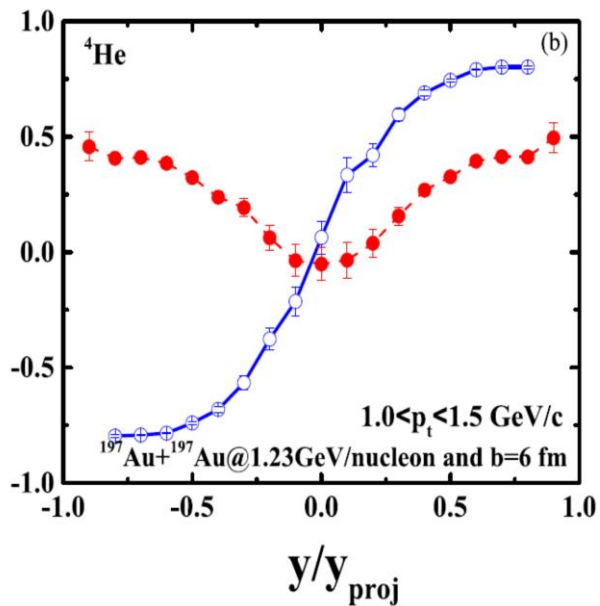
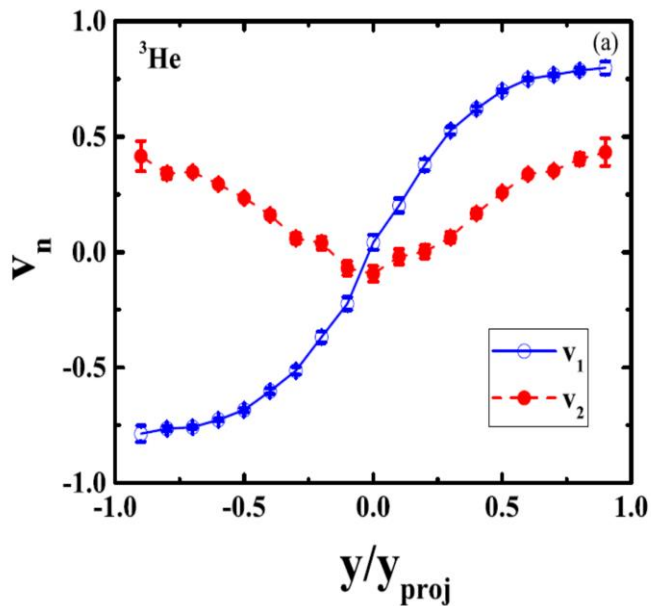
质子和核结团 (d, t, ^3He , α) 集体流

Heng-Jin Liu, Hui-Gan Cheng, Zhao-Qing Feng, Physical Review C 108, 024614 (2023)

$$\frac{dN}{N_0 d\phi}(y, p_t) = 1 + 2v_1(y, p_t) \cos(\phi) + 2v_2(y, p_t) \cos(2\phi) + 2v_3(y, p_t) \cos(3\phi) + 2v_4(y, p_t) \cos(4\phi)$$

$$p_t = \sqrt{p_x^2 + p_y^2}$$

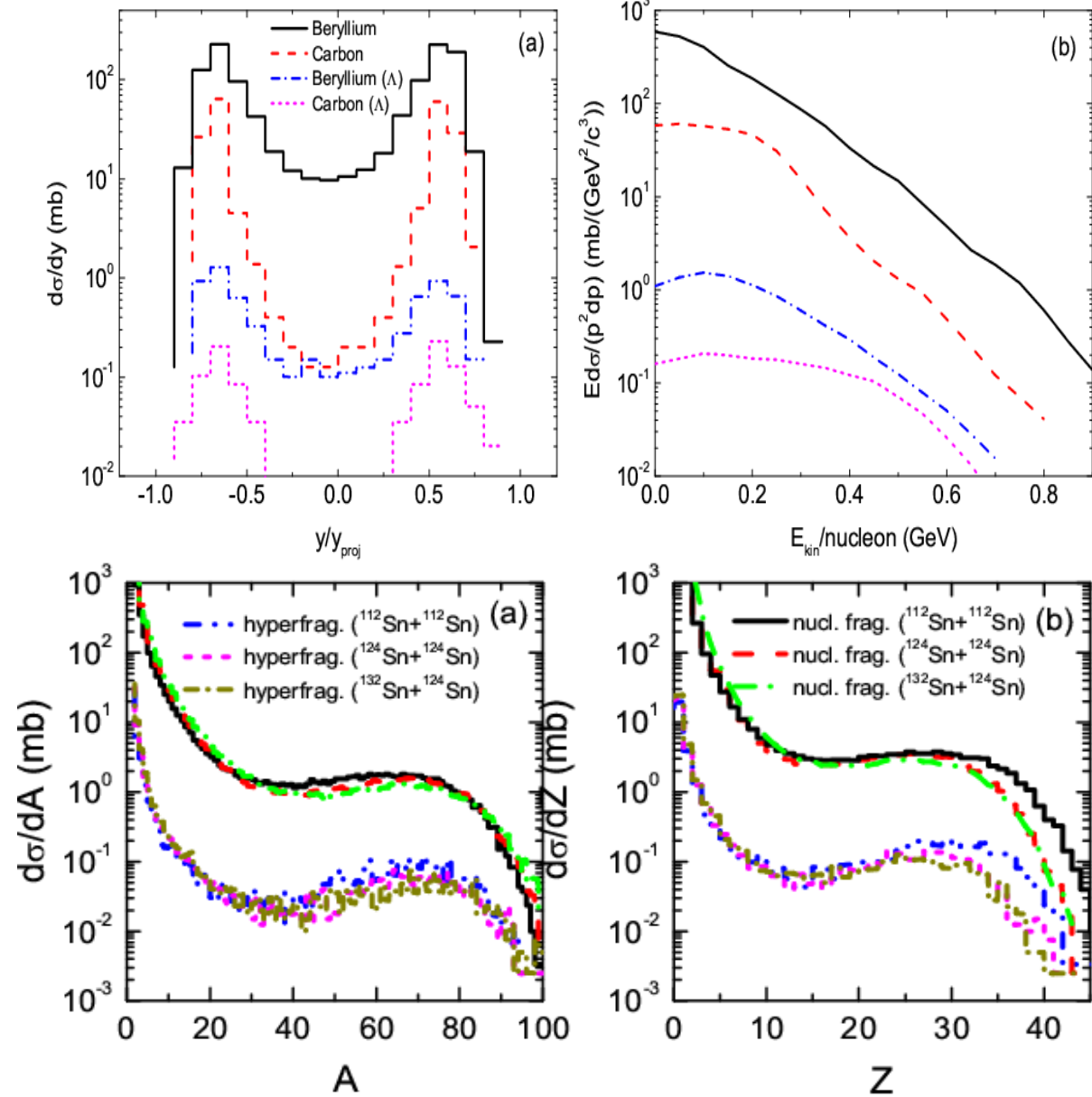
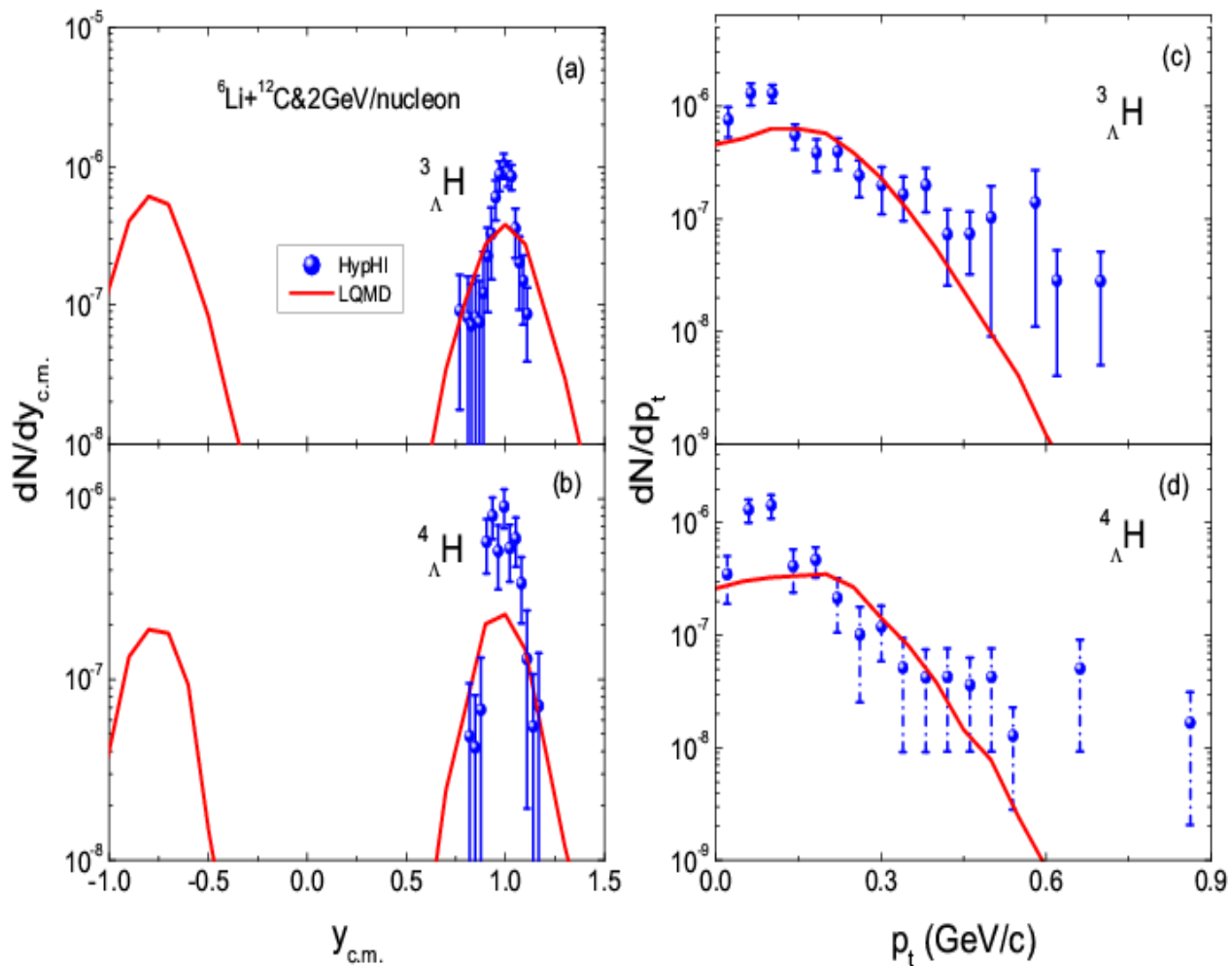
$$y = \frac{1}{2} \ln \frac{E + p_z}{E - p_z}$$



Z. Q. Feng, Phys. Rev. C 102, 044604 (2020)

Data: C. Rappold et al., (HypHI collaboration)

Phys. Lett. B 747, 129 (2015)



Multi-strangeness hypernucleide production

H.G. Cheng, Z. Q. Feng, Phys. Lett. B 824 (2022) 136849

$^{197}\text{Au} + ^{197}\text{Au} @ 3A \text{ GeV}$

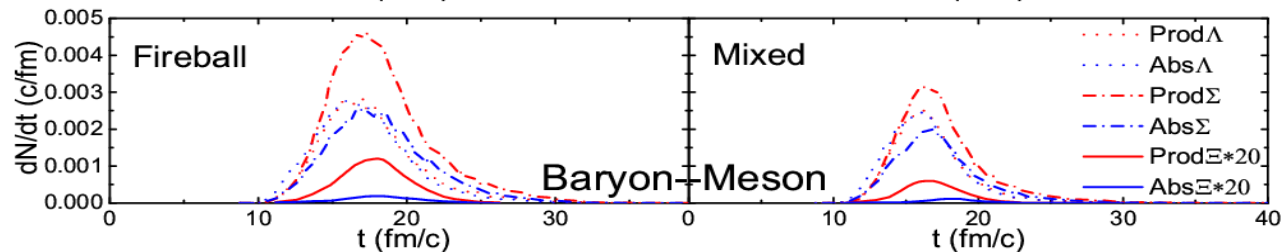
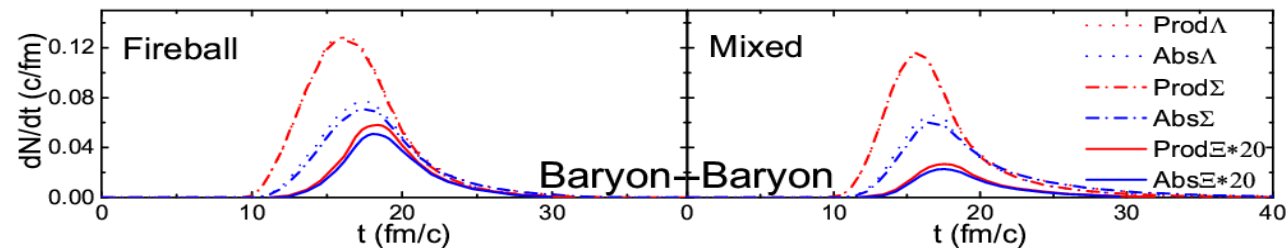
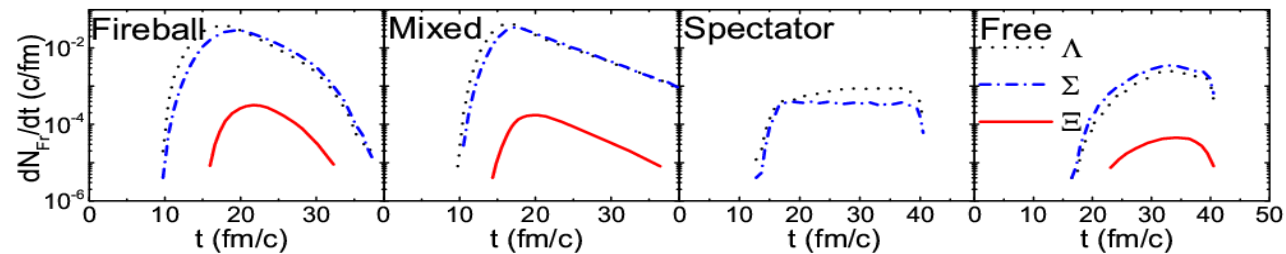
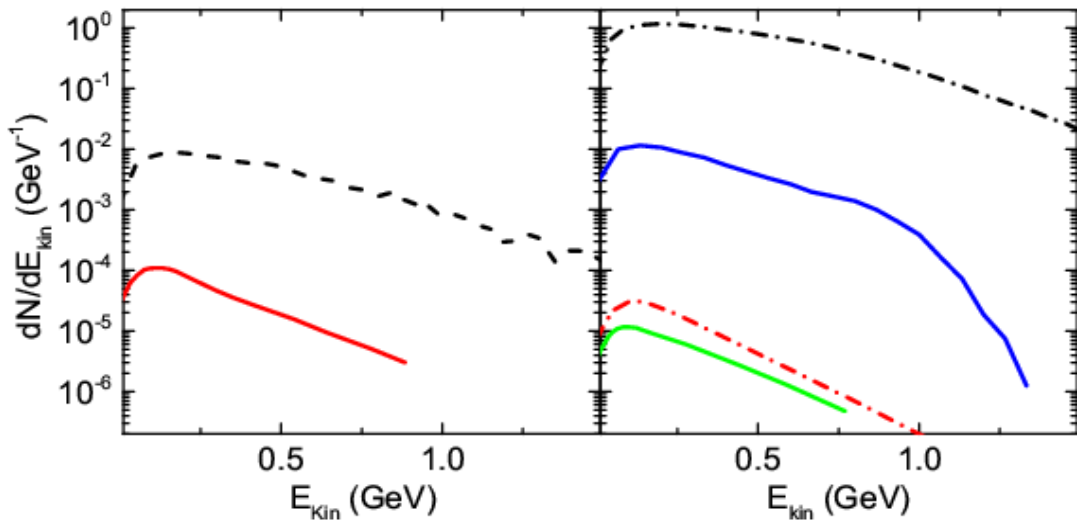
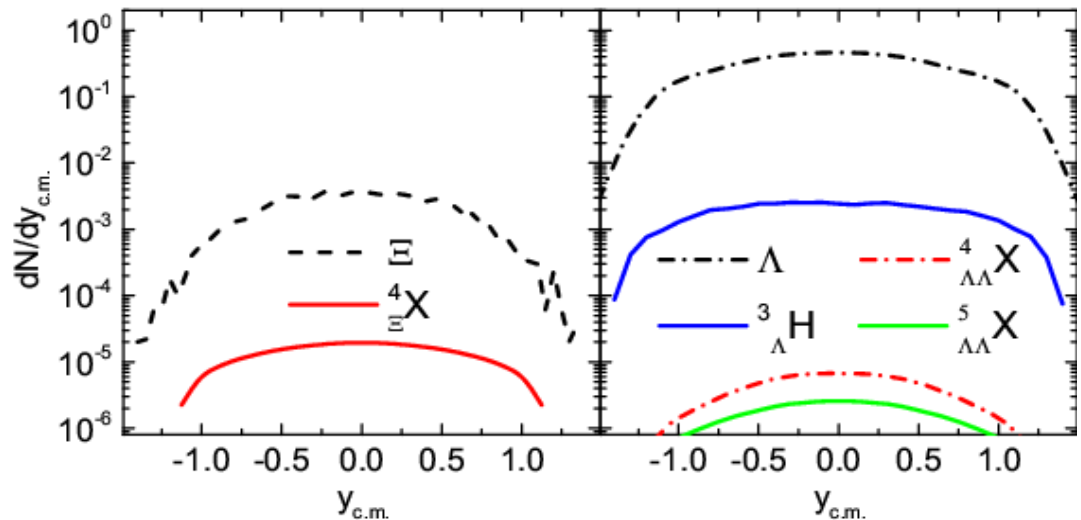
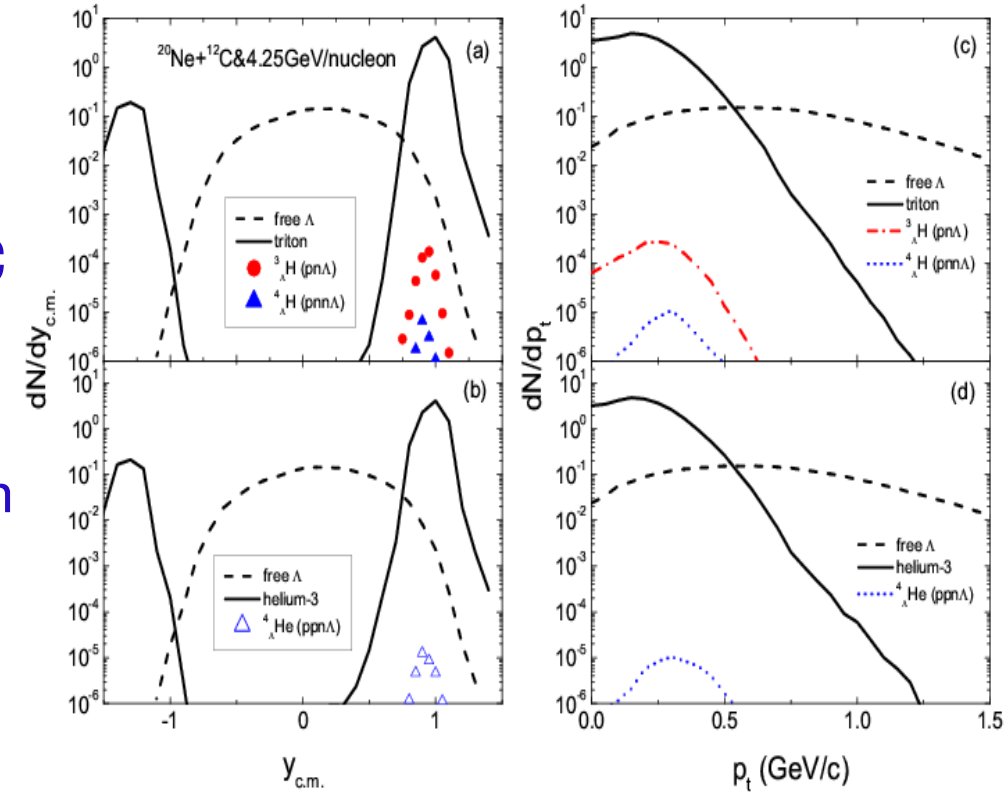


TABLE I. Comparison between cross sections of double lambda hypernuclei calculated with $r_0 = 3.5 \text{ fm}$ for Λ in $^{197}\text{Au} + ^{197}\text{Au}$ and $^{40}\text{Ca} + ^{40}\text{Ca}$ collisions at $3A \text{ GeV}$

Hypernuclei	Cross sections (mb)	
	$^{197}\text{Au} + ^{197}\text{Au}$	$^{40}\text{Ca} + ^{40}\text{Ca}$
${}^4_{\Lambda\Lambda}\text{H}$	2.6×10^{-2}	1.0×10^{-4}
${}^4_{\Lambda\Lambda}\text{He}$	1.0×10^{-2}	$\sim 10^{-5}$
${}^5_{\Lambda\Lambda}\text{H}$	5.9×10^{-3}	$\sim 10^{-5}$
${}^5_{\Lambda\Lambda}\text{He}$	5.1×10^{-3}	$\sim 10^{-5}$
${}^5_{\Lambda\Lambda}\text{Li}$	1.4×10^{-3}	$\sim 10^{-6}$
${}^6_{\Lambda\Lambda}\text{He}$	2.2×10^{-3}	$\sim 10^{-6}$
${}^7_{\Lambda\Lambda}\text{He}$	6.8×10^{-4}	$\sim 10^{-6}$

五、总结

- HIAF重离子碰撞可以产生极端丰中子/丰质子超核、多奇异性超核。入射能量4.25 GeV/核子 $^{20}\text{Ne}+^{12}\text{C}$ 反应可以在HIAF上做超核研究测试实验。
- HIAF能区同位素反应系统 $^{112}\text{Sn}+^{112}\text{Sn}$ 和 $^{124}\text{Sn}+^{124}\text{Sn}$ 中高动能(>0.4 GeV) Σ^-/Σ^+ 双比值(double ratio)可以探针高密对称能。



- HIAF能区重离子碰撞可以提取超子-核子-核子三体相互作用，如 ΛNN , ΣNN , ΞNN 等。
- 超核结团产生涉及多体碰撞、多体关联、Mott效应、超核结合能等。

谢谢大家!